ACS SENSORS

Review

Cite This: ACS Sens. 2018, 3, 903−919

pubs.acs.org/acssensors

Framework-Nucleic-Acid-Enabled Biosensor Development

Fan Yang,[†,‡] Qian Li,[‡] Lihua Wang,[‡] Guo-Jun Zhang,*[,†] and Chunhai Fan*[,‡]

[†]School of Laboratory Medicine, Hubei University of Chinese Medicine, 1 Huangjia Lake West Road, Wuhan 430065, China

[‡]Division of Physical Biology & Bioimaging Center, Shanghai Synchrotron Radiation Facility, Shanghai Institute of Applied Physics, Chinese Academy of Sciences, Shanghai 201800, China

ABSTRACT: Nucleic acids have been actively exploited to develop various exquisite nanostructures due to their unparalleled programmability. Especially, framework nucleic acids (FNAs) with tailorable functionality and precise addressability hold great promise for biomedical applications. In this review, we summarize recent progress of FNA-enabled biosensing in homogeneous solutions, on heterogeneous surfaces, and inside cells. We describe the strategies to translate the structural order and rigidity of FNAs to interfacial engineering with high controllability, and approaches to realize multiplexing for highly parallel in vitro detection. We also envision the marriage of the currently available FNA tool sets with other emerging technologies to develop a new generation of biosensors for precision diagnosis and bioimaging.

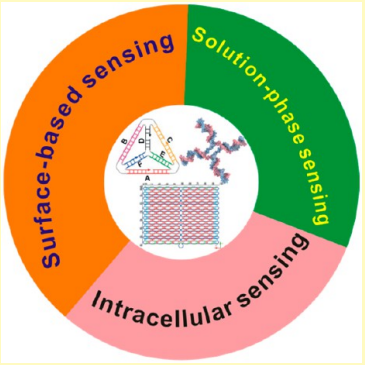

KEYWORDS: *biosensor, DNA nanostructures, framework nucleic acids, in vitro detection, intracellular sensing*

During the passing decades, nucleic acids have been actively exploited to construct various well-defined nanostructures.[1−5] Since the pioneering work on structural DNA nanotechnology by Seeman, we have witnessed the rapid evolution of this highly attractive multidisciplinary field on the boundary of materials, biology, medicine, chemistry, and physics.[6,7] The high precision at the nanoscale and highly predictable Watson−Crick base-pairing rules of DNA hybridization enable tailor-design of virtually any prescribed DNA nanostructures spanning from one-dimensional (1D) to three-dimensional (3D), from symmetry to asymmetry, and from static to dynamic nanoarchitectures.[8−15] By developing "bottom-up" self-assembly strategies, researchers have designed a variety of exquisite DNA structures varying in size and shape, including triangular prism, tetrahedron, polyhedron, DNA tiles, and DNA origami.[16−24] These nanostructures demonstrate important features including intrinsic biocompatibility, structural order, and nanoscale addressability. The availability of these framework nucleic acids (FNAs) shed light on spatially controlled patterning of functional biomolecules at the nanoscale.[25−31]

Biosensors hold great potential for numerous applications including clinical diagnosis, healthcare, environmental monitoring, and homeland defense. However, in vitro biosensors often lack the specificity and sensitivity as seen in their in vivo counterparts. Among many reasons, the reduced target accessibility at the biosensing interface remains a long-lasting hurdle. With the rapid progress in structural DNA nanotechnology, we have seen the availability of various FNAs such as tetrahedron, tile, origami, nanopore, and hydrogel structures that sense targets of interest (Figure 1).[32−42] These biomacromolecular nanostructures possess excellent addressability and high spatial order that can be readily translated to biomolecular signal transduction in various settings (Figure 1). For example, FNA-based scaffolds have been employed to site-specifically anchor small molecules, biomacromolecules, or nanoparticles for electrochemistry- or fluoresence-based signal transduction.[6,30,43−48] More recent advances in FNA-based transmembrane transport have enabled in-cell molecular recognition.[27,49−51] In this review, we aim to summarize recent progress in structural FNA-enabled sensing with particular focus on surface-based sensing, solution-phase sensing, and intracellular molecular recognition.

FNA-ENABLED SOLUTION-PHASE SENSING

Self-assembled DNA nanostructures are usually soluble in solution. By exploiting the addressability of FNAs, researchers have realized site-specific patterning of various types of nanoscale objects ranging from small molecules, biomacromolecules, to nanoparticles, which provides a powerful means to spatially control the ligand−receptor binding at the nanoscale, and/or the signal transduction flow resembling those in in vivo signal pathways.

DNA TETRAHEDRAL NANOSTRUCTURES

By precisely placing fluorescent/quencher molecules in the designated vertices of DNA tetrahedral nanostructures, Zhou et al. recently developed a structure collapse-based "off-on" fluorescent sensor for quantitative analysis of DNA methyltransferase (MTase) activity.[52] Prior to methyl transferring, the

Received: March 27, 2018
Accepted: May 3, 2018
Published: May 3, 2018

DOI: 10.1021/acssensors.8b00257
ACS Sens. 2018, 3, 903−919

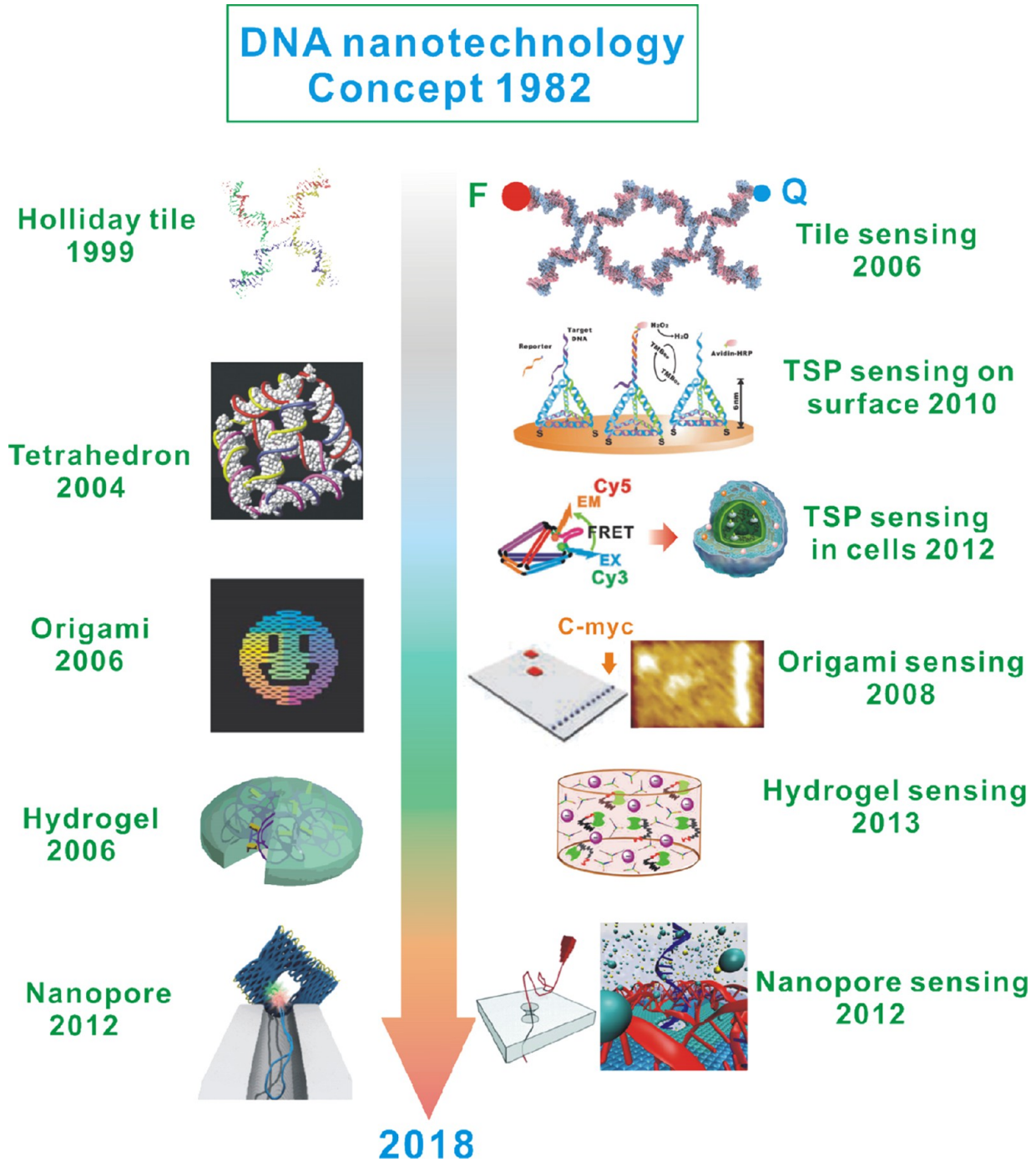

Figure 1. Evolution of DNA nanotechnology-enabled sensing. Holliday tile (Adapted with permission from refs 32 and 33. Copyright 1999 and 2006, respectively, American Chemical Society). DNA tetrahedron (Adapted with permission from ref 34. Copyright 2004, The Royal Society of Chemistry). Tetrahedral structured probe (TSP, adapted with permission from refs 35 and 36. Copyright 2010 and 2012, respectively, Wiley-VCH Verlag). DNA origami (adapted with permission from refs 37 and 39. Copyright 2006 and 2008, Nature Publishing Group and AAAS, respectively). Hydrogel (Adapted with permission from refs 38, 40, and 81. Copyright 2006, 2017, and 2013, Nature Publishing Group and American Chemical Society, respectively). Origami nanopore (Adapted with permission from refs 42, 41, and 75. Copyright 2018, 2012, and 2017, respectively, American Chemical Society).

intact tetrahedral DNA brings fluorophore-quencher tags in close proximity, rendering the nanostructured probe in an "Off" state. Two edges in this tetrahedron were predesigned with recognition site of MTase that could specifically catalyze the methylation of adenosine residues. In the presence of endonuclease DpnI, the methylated sites would be cleaved, resulting in the collapse of tetrahedron structure and the recovery of fluorescence as "On" state (Figure 2a). Using this approach, they achieved a detection limit (LOD) of 0.045 U/mL for MTase and screened multiple methylation inhibitors. Besides, DNA tetrahedra can also be used as a nanoscaffold to spatially load HRP enzymes at three vertices for signal amplification, with one recognition domain at the fourth vertex for target binding in homogeneous solution. In this way, a LOD

DOI: 10.1021/acssensors.8b00257
ACS Sens. 2018, 3, 903−919

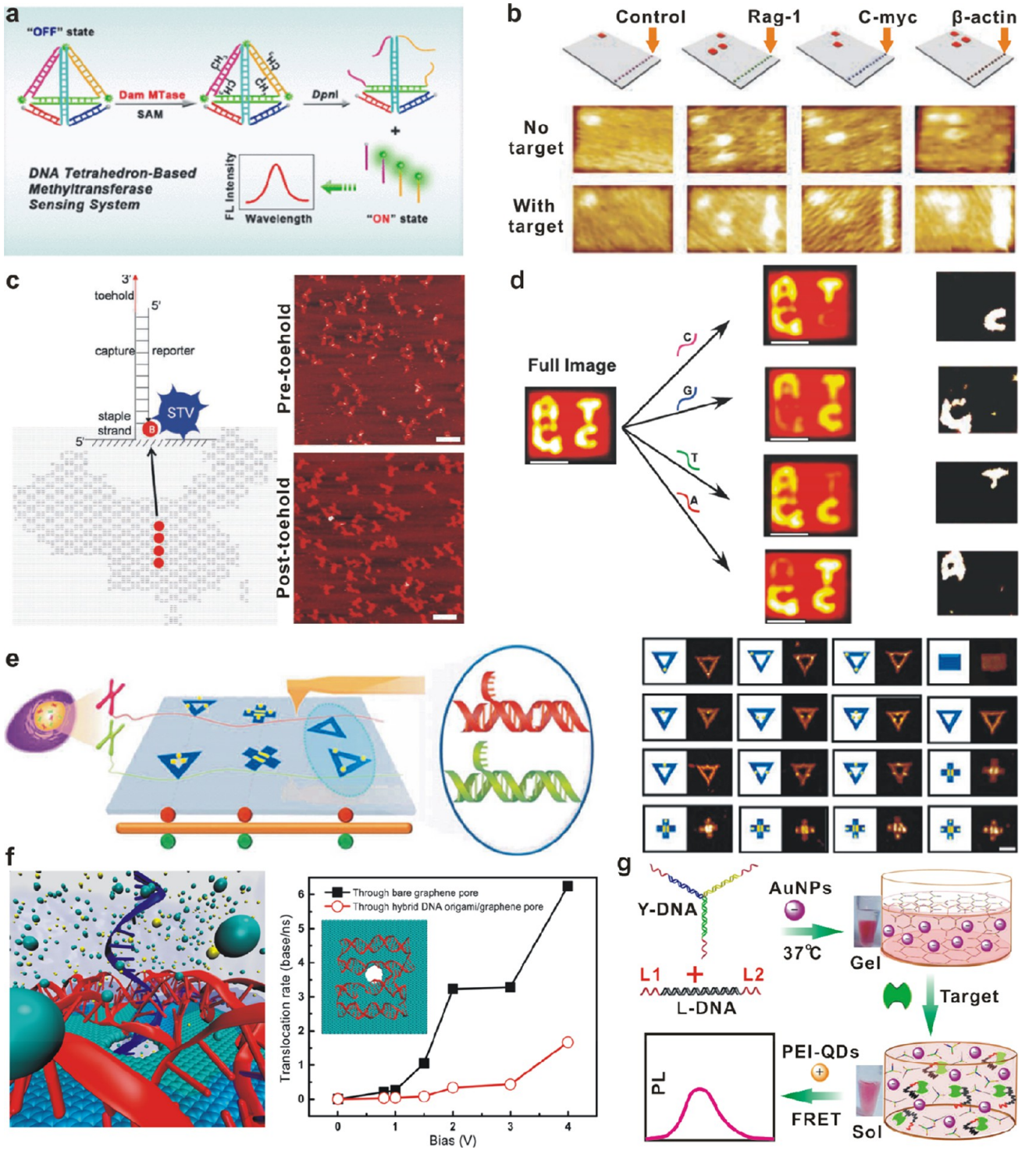

Figure 2. FNA-enabled solution-phase sensing. (a) DNA tetrahedron-mediated quantitative analysis of MTase activity. (b) Symmetric DNA origami tile-based multiplex detection of RNA targets. (c) Asymmetric DNA origami-based toehold-mediated SNP detection. (d) Alphabetic patterned origami structure for SNP detection. (e) DNA origami shape IDs for single-molecule SNP genotyping and haplotyping. (f) DNA origami-graphene hybrid nanopore for ssDNA detection. (g) A switchable DNA hydrogel for thrombin detection through cross-linked Y-DNA and L-DNA tiles. (a, d, f, g) Adapted with permission from refs 52, 59, 75, and 81. Copyright 2017, 2011, 2017, and 2013, respectively, American Chemical Society. (b, c, e) Adapted with permission from refs 39, 58, and 61. Copyright 2008, 2010, and 2017, AAAS, Wiley-VCH Verlag, and Nature Publishing Group, respectively.

down to 10 fM was achieved for a tumor gene fragment using a portable colorimetric assay based on the magnetic bead platform.[53] Further, microRNA (miRNA)-specific TSPs can self-assemble on the gold nanoparticle surface for multiplexed miRNAs analysis.[54] Tetrahedral probes with different dyes were designed to hybridize with the corresponding target miRNA to form DNA/RNA heteroduplex domains. In this design, the fluorescence of vertical dyes would be quenched when approaching the gold surface. By introducing duplex specific nuclease, the DNA part in the heteroduplex could be selectively

DOI: 10.1021/acssensors.8b00257
ACS Sens. 2018, 3, 903−919

digested, which led to the release of dyes and miRNAs. The free miRNA was able to trigger a new round of hybridization-digestion that recovered more fluorescent emissions, resulting in an ultrasensitive detection of three types of target miRNA.

DNA TILE AND ORIGAMI

Two-dimensional DNA nanostructures including DNA tile and origami, which either use crossover design or fold a long viral genome sequence into complex shapes by hundreds of short stapling segments, can act as ideal water-soluble substrates for bioassays.[16,37,55] Double crossover DNA motif is a typical tile element (DX tile), which links two DNA four-way junctions and forms a stiffer helix assembly than routine helices do. Based on DX tile structure, a highly selective nucleic acids sensor was developed, which takes advantage of three adaptor strands that cooperatively complement with target sequence and molecular beacon probe to construct a DX motif-forming sensor.[56] This DX tile sensor conformation is only stable with a fully complementary target molecule, which allows for detection of the analyte with a single-base mispairing. Using precise addressability of DNA nanotechnology, Yan et al. tailored a rectangular DNA tile (60×90 nm^2) for simultaneous detection of multiple RNA targets (Figure 2b).[39] By appending with target-specific probes and built-in "index" sequences at predefined positions, this DNA tile could detect miRNAs (200 pM) in a high background of total cellular RNA. In this process, the formation of stiff DNA-RNA duplex on the tile substrate allows signal detectable with the cantilever of atomic force microscopy (AFM). Such a nanoscale soft DNA chip signifies high promise for single-cell gene expression analysis due to its possible scaling down to a single-cell sample volume.

This symmetrical tile becoming readable exclusively depends on "index" DNA probes that make tile substrate asymmetric. To circumvent this problem, an asymmetric, index-free DNA origami chip was assembled directly into a pattern of Chinese map.[57] The intrinsic asymmetry of the map renders the site of each DNA probe addressable, which would facilitate the imaging analysis by AFM. Using this asymmetric DNA origami platform, Zhang et al. presented a single-nucleotide polymorphism (SNP) genotyping through a toehold-mediated strand-displacement reaction.[58] In the absence of DNA targets, a streptavidin label can specifically absorb on an origami-based biotin-reporter sequence for AFM visualization, whereas the presence of target DNA can induce a toehold-mediated branch migration that releases the streptavidin−reporter complex (Figure 2c). Note that the process of toehold-mediated strand displacement is highly sequence-dependent, which could be effectively terminated by a single-base mismatched strand. Seeman et al. also developed a DNA origami chip for SNP genotyping.[59] This rectangular DNA tile harbors a pattern of alphabetic characters representing the four nucleotides (i.e., A, T, G, and C) that enable AFM imaging with a symbolic display. In the presence of fully complementary sequences, the corresponding toehold probe can trigger branch migration and remove the symbolic character while other toehold-based migrations would be inhibited by a single-base mispair (Figure 2d).

To fully exploit the advantage of origami in nucleic acids assay,[60] a set of DNA origami shape IDs (for example, triangular, cross and rectangular shapes) were self-assembled serving as AFM shape-specific labels for magnified nanomechanical imaging of SNP (Figure 2e).[61] Under AFM imaging, these highly hybridizable origami shape IDs are readily distinguishable, which allow for direct genotyping of human genomic DNA at single-molecule level with a 10 nm resolution. Of note, this origami-based flexible shape design and precise protein patterning provide the possibility to engineer virtually more shape IDs that allow for "multicolored" AFM imaging as compared to fluorescence imaging (usually four colors). Using the high-resolution and "multicolored" imaging capacity of shape IDs, single-molecule genotyping and haplotyping in Han Chinese polulation have been realized. This single-molecule imaging approach was further employed to precisely genotype the hepatitis B virus (HBV) in patients.[62] Despite rapid advances in origami-enabled SNP imaging, the relatively high cost and less multiplexing ability of AFM largely limit its real-world applications.

Apart from origami-based SNP detection, DNA origami tile can also serve as a fully addressable substrate for construction of enzyme pairs and bioreactors.[63] For example, Fu et al. explored enzyme cascade of an enzyme pair using the excellent addressability of DNA origami.[64] They precisely anchored glucose oxidase (GOx) and horseradish peroxidase (HRP) on the surface of a rectangular DNA origami with interenzyme spacing from 10 to 65 nm. The distance-dependent enzymatic kinetics revealed that the smaller spacing would facilitate the enzyme cascade. Similarly, the GOx-HRP pair has also been immobilized on a rapidly assembled DNA origami with sub-10 nm resolution, in which bienzyme cascade efficiency was enhanced by rolling the rectangular origami into a nanotube.[65] The promoted catalytic activity is synergistically contributed by the stabilizing function of DNA nanostructure and the nanoconfined caging effect.[66] Of note, the product of rolling circle amplification (RCA) could be folded into a DNA origami nanobelt by staple strands for immobilization of numerous enzymes.[67] In combination with magnetic bead-based ELISA, this DNA nanoprobe is capable of detecting PSA down to 50 aM.

DNA ORIGAMI NANOPORE

DNA origami nanostructures can use their precise control over geometry and surface functionality to construct DNA nanopores that either form sophisticated hybrid structures with solid-state nanopores or embed into lipid bilayers for biomolecule sensing.[68] Usually, solid state nanopores permit tunable pore sizes that are useful for testing large biomolecules (e.g., dsDNA and proteins), but they are limited by the uncontrollable surface functionality (for example, precise positioning single binding sites for analytes). In contrast, the biological nanopores, such as the most widely used α-hemolysin, largely outperform their solid-state counterparts in surface functionality via genetic engineering, whereas their narrowest dimension are often less than 2 nm that exclusively allows detection of single-stranded (ss)DNA or small molecules.[69]

In this context, DNA origami nanopores may provide a route to address the challenge since it enables the construction of size-tunable biological nanopores and precise anchoring of the target-responsive probes.[70,71] DNA origami nanopores have been exploited to either synergize solid state nanopores for engineering hybrid architectures or directly insert into a synthetic lipid membrane channels with hydrophobic functionalization for translocation of DNA hairpins and dsDNA analytes.[41,72−74] For example, a hybrid graphene−origami nanopore was developed for DNA detection.[75] This heterostructured nanopore is highly functionalized and allows

DOI: 10.1021/acssensors.8b00257
ACS Sens. 2018, 3, 903−919

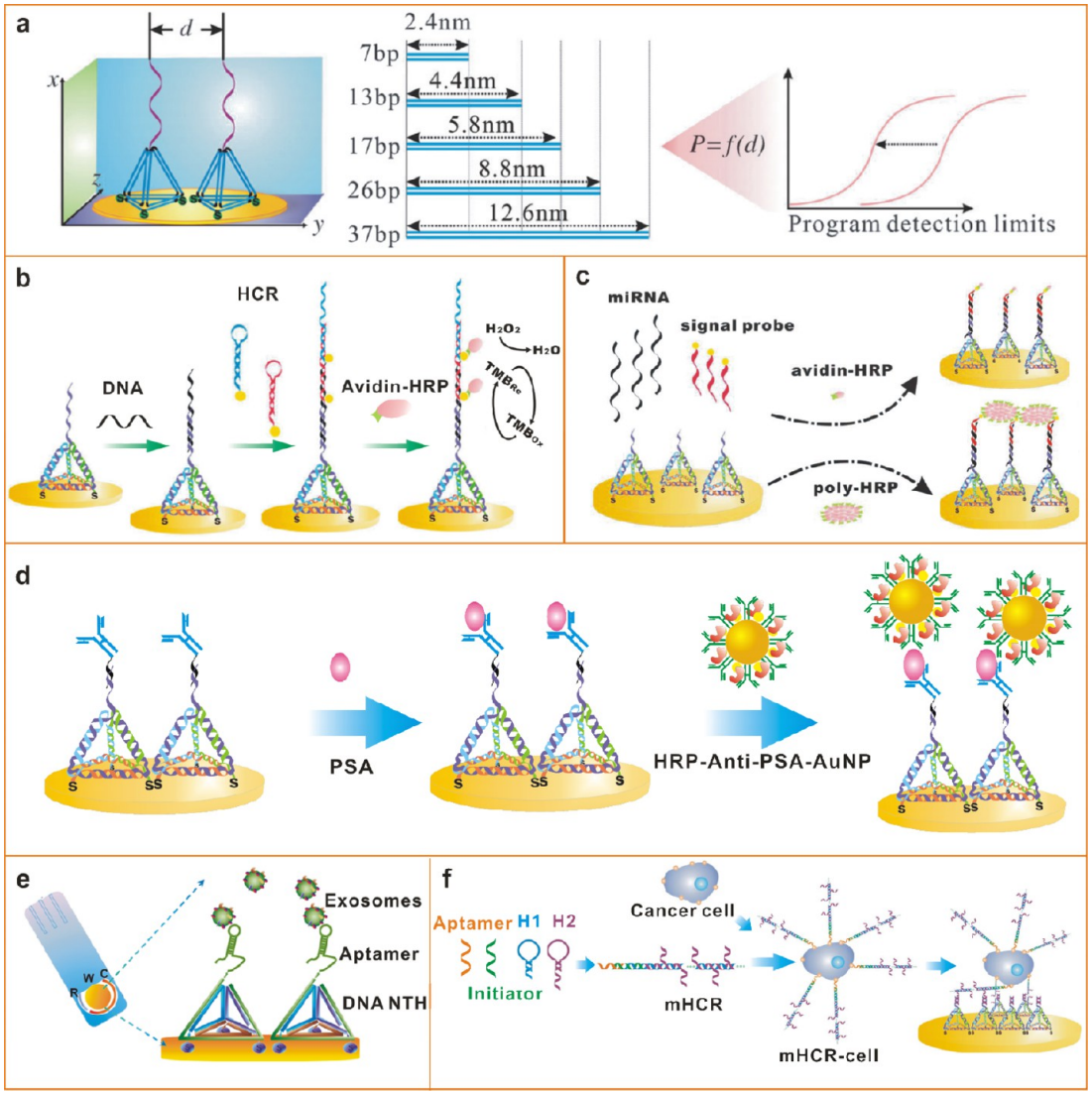

Figure 3. DNA tetrahedron-based electrochemical biosensors (eTSP-sensors). (a) DNA tetrahedrons varying in size for programmable DNA detection (Adapted with permission from ref 48. Copyright 2015, Wiley-VCH Verlag). (b) Hybridization chain reaction coupling eTSP-sensor for signal-enhanced DNA detection. (c) eTSP-sensor for microRNA detection (adapted with permission from ref 100. Copyright 2012, Nature Publishing Group). (d) eTSP-sensor conjugated antibody for PSA detection with HRP-AuNP amplification. (e) eTSP-sensor conjugated aptamer for sensitive exosome detection. (f) eTSP-sensor conjugated aptamer-HCR for detection of cancer cells. (b, d–f) Adapted with permission from refs 90, 107, 115, and 116. Copyright 2014 and 2017 American Chemical Society.

unpaired T bases to dangle at the mouth of graphene pore for monitoring DNA translocation. In this design, the DNA origami would attach to the graphene with well-alignment under negative bias, which benefits the controlled signals readout. With these advantages, this hybrid nanopore contributes to a longer residence time of single base and slower translocation of ssDNA through nanopore and thereby yields a higher resolution of signal acquisition over its bare graphene counterpart (Figure 2f).

DNA HYDROGELS

DNA hydrogels are macroscopic gels and cross-linked by unusual DNA nanostructures, which are often created by enzymatic polymerization cooperated with intermolecular i-motif structures.[40,76−79] In this way, a typical DNA meta-hydrogel was synthesized by RCA and multiprimed chain amplification.[80] This water-sensitive hydrogel could detect electric-current switch. To realize biomolecular detection, Lei et al. developed a switchable DNA hydrogel using Y-shaped DNA tiles (Y-DNA) and aptamer linker DNA units (L-DNA).[81] L-DNA contains a thrombin-responsive aptamer sequence (L1) and a Y-DNA complementary domain (L2). Without thrombin, the two building blocks (Y-DNA and L-DNA) can cross-link to a functional hydrogel that forms a rigid space to encapsulate gold nanoparticles (AuNPs) as a visual agent. Upon adding thrombin, the hydrogel structure would quickly collapse and release the trapped AuNPs for visual detection because of the specific binding with the L1 aptamer. Next, the free negatively charged AuNPs can approach the positively charged QDs to develop a FRET-based fluorescence-quenching strategy for thrombin detection (Figure 2g). Beyond biomolecules and ions, larger-size circulating tumor cells (CTCs) have also been analyzed with DNA hydrogels. To achieve this, the porous DNA hydrogels assembled with an aptamer-trigger clamped HCR were used for CTC identification, cloaking and decloaking analysis.[82] After specific recognition of CTC surface

DOI: 10.1021/acssensors.8b00257
ACS Sens. 2018, 3, 903−919

marker, the aptamer-toehold strand can induce an effective HCR to form porous hydrogel that allows for cloaking the target CTC. In the presence of chemical stimuli, the captured living cells could be released from the hydrogel for subsequent live cell analysis.

Instead of DNA strands-cross-linked hydrogel, nucleotides, like guanosine (G), can also self-assemble into nanofibrous hygrogel assisted by $KB(OH)_4$ that guides the formation and stacking of cation-templated G-quartet motifs.[83] By incorporating hemin into G_4-motif, the hydrogel would evolve into having peroxidase-like activity that catalyzes in situ deposition of conducting polyaniline on G-quartet scaffold. Pei and coworkers thus printed such a conductive G-quartet hydrogel with embedded GOx on flexible electrode surface to develop an enzyme sensor. This artificial G_4-enzyme hydrogel also allows for highly sensitive detection of Pb^{2+} by measuring the Pb^{2+}-triggered enzymatic activity loss of the hydrogel.[84] Compared to K^+, Pb^{2+} shows higher efficiency to stabilize G_4. Pb^{2+} thus can replace K^+ and induce the release of hemin that contributes to the decrease of enzyme activity because of a conformational interconversion in hydrogel. Using this strategy, Li et al. achieved a LOD of Pb^{2+} down to 0.32 pM.

FNA-ENABLED SURFACE-BASED SENSING

The structural order and precision of DNA nanostructures render their ability to engineer sensing interface in solid-state sensors. Taking DNA tetrahedron as an example, the design of which was first reported in 2004, it has become an increasing important biomolecular scaffold in interface engineering.[26] As compared to linear single-stranded or duplex DNA probe, tetrahedron structured probe (TSP) has several advantages in engineering of biosensing interface. First, TSP is mechanically rigid enough to adopt an ordered and upright orientation at the surface. Second, the TSP-modified surface is protein-resistant, which allows the TSP-based sensors to be used directly in complex matrices, such as biofluids. Third, 3D TSP structures not only spatially segregate neighboring probes avoiding molecular entanglements but also place the probes in a solution-phase-like setting to minimize surface effects. Moreover, molecular diffusion and convection at TSP-decorated interfaces are also expected to be faster than those at smooth macroscopic ones, which are significant for improving sensitivity of sensors.[85] These merits render TSP an attractive functional scaffold that has a wide application in electrochemical and optical biosensing.[50]

ELECTROCHEMICAL DETECTION

By modifying thiol groups (−SH) at three vertices of TSP, a typical electrochemical TSP would be formed, in which a pendant domain serves as recognition probe at the fourth vertex and the three −SHs can firmly anchor on gold electrode surface via Au−S chemistry.[35] As compared to the single −SH, the three thiolated DNA strands are able to increase the stability of the surface-confined TSP by several thousand folds.[86] In a TSP-based electrochemical sensor, the lateral interprobe spacing is predominantly controlled by the size of tetrahedron scaffold.[87] Lin et al. designed multiple TSPs with side length ranging from 2.4 to 12.6 nm to tune the probe distance (Figure 3a).[48] They found an inverse proportion between TSP density and size that was also linearly related with lateral distance of TSP. Using this approach, they can program the sensitivity of the sensor (1 fM - 10 pM) and achieve a low detection limit of 1 fM for target DNA molecules. This typical sandwich detection format enabled a highly sensitive and sequence-specific detection of a gene fragment of avian influenza A (H7N9) virus.[88] In combination with poly-HRP, this sensor was able to read out *E. coli* genome as low as 0.2 pg/μL.[89] Coupling with hybridization chain reaction (HCR) mediated signal amplification, this electrochemical TSP sensor (eTSP-sensor) can further improve the sensitivity to 100 aM in DNA detection (Figure 3b).[90] Recently, Zhao et al. integrated eTSP-sensor with asymmetric methylation-specific PCR pushing the detection limit of methylated DNA to single copy level.[91] Of note, since Pei et al. first employed TSP-patterned gold electrodes to quantify DNA target and discriminate the mismatched sequences,[35,92] such an eTSP-sensor was quickly extended to detect a variety of targets of interest beyond DNA.[25,93−96]

Various miRNAs have been readily detected using eTSP-sensors based on the identical base-pairing properties as DNA sequences.[97,98] For example, a target-responsive TSP with a pendant stem-loop was developed to specifically hybridize with miR141.[99] The free domain in opened stem-loop was subsequently flanked by the biotinylated reporter probe in a sandwich way. This assembly structure amplified electrochemical signal via the substrate catalysis of HRP, yielding a LOD down to 1 fM. Likewise, Wen et al. used interfacial engineering and multienzyme amplification strategy to achieve an extremely low LOD of 10 aM in miRNA quantitation (Figure 3c).[100] In addition to enzymatic amplification, eTSP-sensor is prone to integrate with nonenzymatic HCR or RCA,[101] and has been used as template for arranging a linear silver nanoparticle array in tandem.[102−104] Impressively, such a highly sensitive eTSP-RCA sensor can push the LOD down to 2 aM.[102] As compared to these single signal readouts, a multiplexing eTSP-sensor array is capable of profiling multiple miRNAs targets simultaneously. A disposable screen-printed gold electrode array (16-channel) with sequence-specific TSPs was tailored to detect four types of miRNAs associated with pancreatic carcinoma at femtomolar levels.[105]

Besides, the DNA tetrahedron structure can also link antibodies to form an electrochemical immunorecognition layer. Pei et al. first anchored TNF-α onto TSP surface for building a regenerable eTSP-sensor via DNA-bridged antibody conjugation, which easily probed 100 pg/mL of TNF-α.[106] Later, click-chemistry-based antibody conjugation strategy was used to immobilize the antibody of prostate-specific antigen (PSA) on a TSP scaffold (Figure 3d).[107] By precise spacing of antibodies using a rigid scaffold, a very high sensitivity (1 pg/mL) was achieved in PSA detection. Instead, Leong et al. introduced a DNA-bridge-free approach to tether anti-IgG or anti-*E. coli* antibody on TSP via EDC-NHS chemistry for ultrasensitive antigen and bacteria detection.[108−110]

By designing the pendant probe with functional nucleic acids, such as aptamers, this eTSP sensor is capable of measuring small molecules, ions, exosomes, and cells. For example, a split aptamer for cocaine was incorporated into TSP to build a signal-on electrochemical sensor, which achieved a remarkable high sensitivity (33 nM) in cocaine detection.[111] Similarly, Yin et al. designed an anti-ATP aptamer at the TSP top to develop an ATP-responsive sensor that uesd $Ru(phen)_3^{2+}$ intercalation to realize a sensitive readout of ATP (0.2 nM).[112] They also constructed a turn-on Hg^{2+} sensor using TSP-scaffolded mercury-specific functional oligonucleotide and achieved a LOD of 100 pM.[113] Different from this single-point probe

DOI: 10.1021/acssensors.8b00257
ACS Sens. 2018, 3, 903−919

Table 1. Comparison between the Proposed eTSP Sensors for Bioassays

signal amplification[a]	target[b]	readout[c]	dynamic range	LOD	ref
HRP/TMB	DNA	i-t	1 pM to 10 nM	1 pM	35
HRP/TMB	DNA	i-t	1 fM to 0.1 nM	1 fM	48
HRP/TMB	H7N9 gene	i-t	1 pM to 0.1 μM	0.1 pM	88
poly-HRP/TMB	*E.coli* genome	i-t	0.2−200 pg/μL	0.2 pg/μL	89
HCR/HRP/TMB	DNA	i-t	1 fM to 0.1 nM	0.1 fM	90
PCR/HRP/TMB	methylated DNA	i-t	3−150 pg	3 pg	91
AuNP/graphene	NADH	DPV	1 fM to 100pM	1 fM	93
HRP/TMB	telomerase activity	i-t	0−5 × 10^4 cells	10 cells	94
L-AuNP/CdS	telomerase activity	ECL	1−90 × 10^{-8} IU	2 × 10^{-9} IU	96
hemin/G4/PANI	8-OHdG	DPV	10 pM to 2 nM	1 pM	95
G wire/TMB	miR21	i-t	0.5−10 nM	176 nM	98
HRP/TMB	miR141	i-t	1 fM to 1 nM	1 fM	99
poly-HRP/TMB	miR21	i-t	10 aM to 1 nM	10 aM	100
HCR/HRP/TMB	miR122b	i-t	10 aM to 1 pM	10 aM	90
enzyme/AgNP	miR21	LSV	1 fM to 1 nM	0.4 fM	103
RCA/AgNP	Let-7a	LSV	0.1fM to 10 nM	50 aM	104
HCR/AuNP/AgNP	miR175p	LSV	0.1 fM to 0.1 nM	2 aM	102
poly-HRP/TMB	miR21,155,196a,210	i-t	10 fM to 1 nM	10 fM	105
HRP/TMB	TNF-α	i-t	0.1−5 ng/mL	0.1 ng/mL	106
HRP/TMB	PSA	i-t	1−100 pg/mL	1 pg/mL	107
FeC-Ab	IgG	SWV	0.01−100 ng/mL	2.8pg/mL	108
FeC-Ab	*E.coli* LPS	SWV	0−3 ng/mL	0.2 ng/mL	109
FeC-Ab	PspA peptide	SWV	K	0.2 ng/mL	110
HRP/TMB	cocaine	i-t	0.1 μM to 1 mM	33 nM	111
$Ru(phen)_3^{2+}$	ATP	ECL	0.5 nM to 1 μM	0.2 nM	112
MB	Hg^{2+}	DPV	0.1−20 nM	100 pM	113
MB	ATP	SWV	1 nM to 1 μM	5 nM	114
$[Fe(CN)_6]^{3-/4-}$	exosome	SWV	10^5−10^{12}/mL	2 × 10^4/mL	115
HRP/TMB	MCF-7 cells	i-t	0−10^3 cells	4 cells	116

[a]L-AuNP, luminol gold nanoparticle; hemin/G4/PANI, hemin/G-quadruplex and polyaniline; G wire, guanine nanowire; FeC-Ab, ferrocene-antibody. [b]NADH, dihydronicotinamide adenine dinucleotide; 8-OHdG, 8-hydroxy-20-deoxyguanosine; *E. coli* LPS, *E. coli* lipopolysaccharides; PspA peptide, pneumococcal surface protein A peptide. [c]DPV, differential pulse voltammetry; ECL, electrochemiluminescence; LSV, linear sweep voltammetry; SWV, square wave voltammetry.

design, another type of TSP was tailored with two split halves of ATP aptamer appended to two vertices respectively (one is at TSP top).[114] With this design, a single-step detection of ATP at nanomolar level was achieved. Inspired by these advantages of TSP scaffold, Wang et al. recently engineered an eTSP-aptasensor for direct capture and detection of tumor exosomes (Figure 3e).[115] This aptasensor showed improved target accessibility and higher sensitivity (2.09 × 10^4 exosomes/mL) as compared to the ssDNA-counterpart. To perform highly sensitive detection of biological objects with larger size, such as cancer cells, a synergic TSP-aptamer interface was engineered using multibranched HCR that offers multiple biotins and branched arms for multivalent capture and signal amplification (Figure 3f).[116] These successful applications of eTSP-sensor in ultrasensitive bioassays have proved the unique advantages of DNA nanostructures in electrochemical interface modulation and sensitivity improvement (Table 1).

OPTICAL DETECTION

As a versatile molecular scaffold, TSP is also compatible with optical detection modes, such as glass-based fluorescence analysis. Using commercially available nucleotide modifications, a variety of functional groups beyond −SH could be conjugated to oligonucleotides for synthesis of specific TSP.[86] Amine group modification facilitates TSP to be anchored on glass slide surface for single molecule detection through epoxy-amine reaction.[117] In this approach, quantum dots (QDs) were captured as fluorescent probes on TSPs via target-induced streptavidin−biotin binding. By imaging with epifluorescence microscopy, a digital counting of dots was realized for single DNA molecules readout (Figure 4a). Replacing the pendant linear DNA with a stem-loop structure that has a toehold domain, this QDs-based single-molecule imaging platform enabled a toehold-mediated sensitive detection of miRNA with LOD down to 5 fM.[118] To realize the detection of microRNA at single molecule level, Wang et al. developed a plasmonic nanobiosensor that used single TSP-modified Au@Ag core−shell nanocube as a plasmonic probe to capture target microRNA and meanwhile induced the signals of localized surface plasmon resonance (LSPR).[119] Using this nano-plasmonic sensor, a single miRNA21 binding event can generate ∼4 nm wavelength shift of LSPR scattering spectral. Such a high sensitivity allows ultrasensitive detection of microRNA and logic operation (Figure 4b). Instead of direct anchoring on sensor surface, TSP could also be used as a nanolabel for signal amplified quantitative detection of HIV-related DNA and human IgG, particularly at the single-molecule level.[120,121] Besides, TSP can amplify the optical signals in biolayer interferometry by enlarging the sensing interfacial thickness or density.[122] This TSP-enhanced dip-and-read method allowed a label-free and sensitive detection of DNA and ATP respectively. Further, TSP coupling with dual

DOI: 10.1021/acssensors.8b00257
ACS Sens. 2018, 3, 903−919

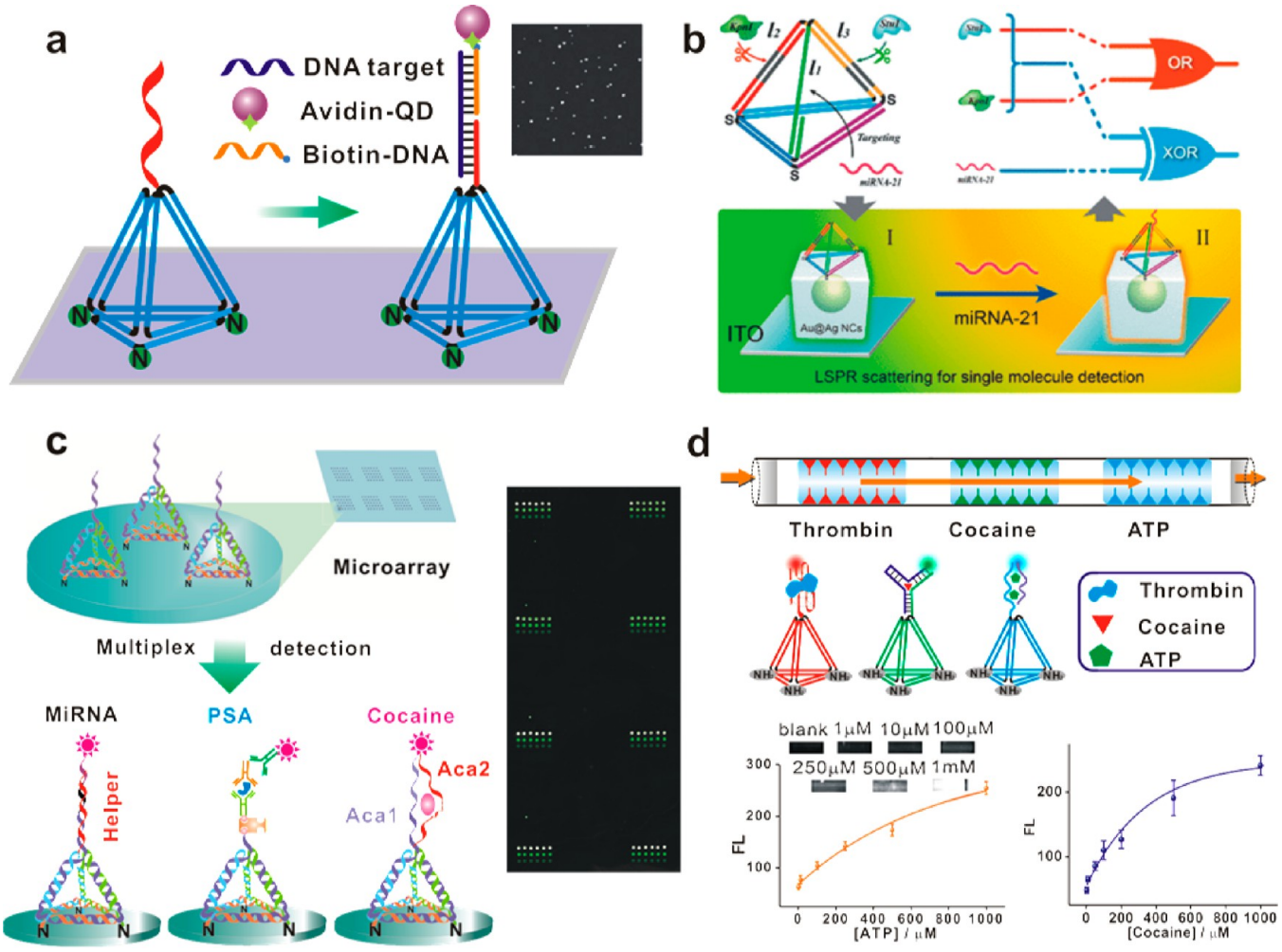

Figure 4. TSP-based optical detection on surface. (a) TSP-based epifluorescence imaging of single DNA molecule using QDs as reporter (Adapted with permission from ref 117. Copyright 2012, The Royal Society of Chemistry). (b) TSP-based plasmonic biosensor for single molecule analysis of microRNA21. (c) TSP-based microarrays for multiplex detection of let-7a, PSA and cocaine. (d) TSP-mediated capillary microarray for multiplexed bioassays of thrombin, ATP and cocaine. (b–d) Adapted with permission from refs 119, 124, and 125. Copyright 2018, 2014, and 2017, respectively, American Chemical Society.

polarization interferometry technique enabled a real-time monitoring of the interactions between TSP-scaffolded G-rich sequences and Pb^{2+} ions and realized a label-free, sensitive determination of Pb^{2+} (9 nM).[123]

In addition, TSPs could be easily incorporated into a microarray platform for multiplexed targets readout by substituting the pendant recognition domain with the corresponding target-responsive probes. Li et al. engineered an addressable microarray by covalently linking amine-TSPs onto aldehyde-glass chips for multiplex detection of let-7a, PSA, and cocaine with improved sensitivity and specificity (Figure 4c).[124] To accelerate the target binding, a DNA nanostructured aptamer pull-down approach was developed for a quick and arrayed assay in a glass capillary.[125] This TSP-based pull-down assay allowed for multiplexed and sensitive fluorescent detection of the contents (ATP, cocaine and thrombin) in droplets with nano- or picoliter volumes (Figure 4d). They further constructed a bubble-mediated DNA nanostructured capillary microarray that enabled a rapid and multiplex quantitation of three heavy-metal ions (i.e., Ag^{+}, Hg^{2+}, and Pb^{2+}) at the nanomolar level.[126] These results demonstrate that TSPs have higher sensitivity, which is in agreement with the report by Howorka and coauthors.[127] Importantly, a single molecular probe can be precisely anchored on a single tetrahedron structure to form single nanostructured probes, which is difficult to realize on inorganic nanostructures. Moreover, incorporating nanostructured FNAs onto macroscopic surface offers a route to engineering trans-scale biosensing interface for enhanced molecular recognition, which ultimately benefits surface-based biosensors.[48]

FNA-ENABLED INTRACELLULAR SENSING

DNA nanostructures can serve as idea carrier platforms to delivery cargos (e.g., functional molecules and drugs) into cell for diagnostic and therapeutic applications. The quantitative analysis of cellular biomolecules and metabolites with high spatial-temporal resolution can assist the elucidation of molecular mechanism and heterogeneity in living cells at single-cell level. Compared with other molecular carrier, DNA nanostructures have several unique merits for intracellular molecular detection. First, negatively charged DNA nanostructures facilitate transfection-free endocytotic internalization through receptor-mediated transmembrane transport. Second, the internalized nanoscaffold would dock in cytoplasm and thus

DOI: 10.1021/acssensors.8b00257
ACS Sens. 2018, 3, 903–919

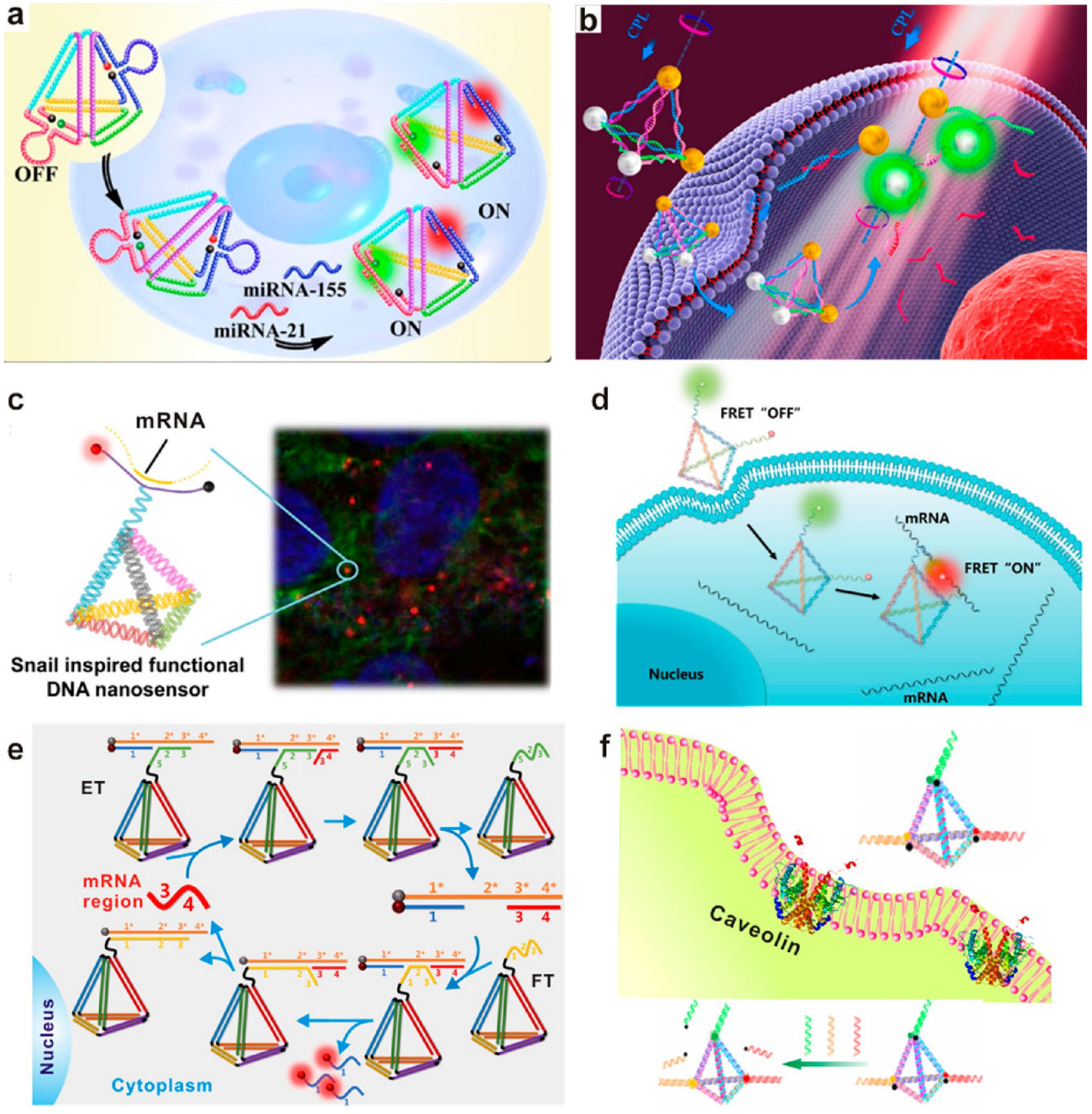

Figure 5. FNA-enabled intracellular RNA sensing. (a) Dual-color encoded reconfigurable DNA nanoprobe for simultaneous imaging of two intracellular miRNAs. (b) DNA pyramid-mediated chiroptically active nanoassembly for dual-mode miR21 detection. (c) TSP-based nanosensor for GAPDH mRNA detection. (d) DNA nanotweezer-based FRET strategy for detection of TK1 mRNA in cells. (e) Entropy-driven tetrahedron-based amplifier for sensitive detection of intracellular TK1 mRNA. (f) Multicolor-encoded tetrahedral nanoprobes for simultaneous detection of multiple mRNAs in cells. (a–f) Adapted with permission from refs 131–135 and 137. Copyright 2016, 2015, 2018, and 2017, respectively, American Chemical Society.

enables molecular recognition inside different cellular compartments. Third, DNA nano-objects, like tetrahedrons, are enzymatically resistant, which allows them to retain the intact structure during intracellular transport.[128,129] Fourth, the natural DNA scaffold has intrinsic biocompatibility and does not exhibit cytotoxicity. Based on these advantages, DNA nanoarchitectures have been widely delivered into cells for precise molecular recognition and detection of nucleic acids and non-nucleic acid targets.

NUCLEIC ACIDS SENSING

The concentration variation and spatiotemporal distribution of intracellular nucleic acids are closely associated with the state of living cells and disease progression. However, accurate probing of these dynamic processes in cells remains challenging. To address this, multiple DNA nanostructures designed with target-responsive elements have been developed for precise detection of nucleic acids (e.g., miRNA and mRNA) in cytoplasm. Inspired by the reconfigurable design of DNA

DOI: 10.1021/acssensors.8b00257
ACS Sens. 2018, 3, 903–919

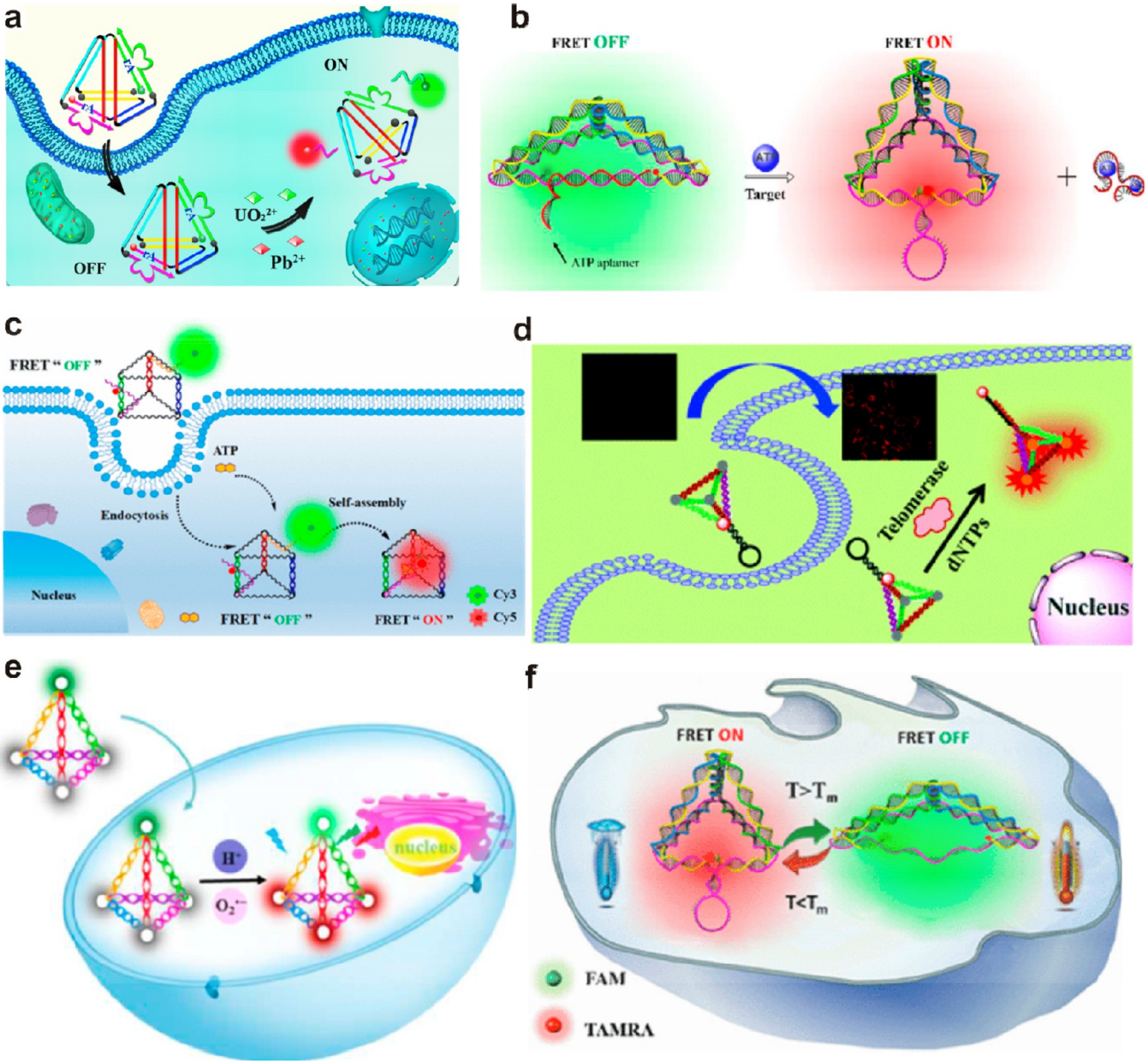

Figure 6. FNA-enabled intracellular sensing of non-nucleic acid targets. (a) Dual-color encoded DNA nanoprobe for multiplexed detection of intracellular toxic metal ions (Adapted with permission from ref 138. Copyright 2016, Elsevier). (b) Competition strand-mediated DNA tetrahedral probe for detection of intracellular ATP molecules. (c) DNA nanoprism-based split aptamer for intracellular ATP sensing. (d) AuNP-based tetrahedral FRET probe for "off-on" fluorescent readout of telomerase activity in cells (Adapted with permission from ref 141. Copyright 2018, The Royal Society of Chemistry). (e) DNA tetrahedral probe enabling simultaneous detection of pH and $O_2^{\bullet-}$ in cells. (f) Scallop-inspired, thermosensitive DNA nanothermometer probing intracellular temperature change. (b, c, e, f) Adapted with permission from refs 139, 140, 142, and 143. Copyright 2016 and 2017, respectively, American Chemical Society.

tetrahedron and its intracellular logic operation,[36,130] Xiang et al. developed a dual-color-encoded reconfigurable tetrahedron nanoprobe for simultaneous imaging of two miRNAs within living cells.[131] In this design, two folded hairpin domains that could specifically recognize the target miR-21 and miR-155 were separately incorporated into two different edges. Meanwhile, two fluorophore-quencher pairs were respectively located close to the two hairpin sequences. The rigid tetrahedron structure permits fluorophore/quencher pairs in close proximity, which quenches the fluorescence emission. In the presence of target miRNAs, the corresponding hairpin structure would unfold and separate the fluorophores from the quenchers, thus recovering the fluorescence signal for "signal-on" readout of target miR-21 and miR-155 in MDA-MB-231 cells, respectively (Figure 5a). Different from this TSP-based fluorescent dyes-driven miRNA sensing, high-photostability nanoparticles, such as AuNPs and upconversion nanoparticles (UCNPs), could also been incorporated into DNA frame for ultrasensitive quantification of intracellular miRNA. To achieve this, Xu et al. assembled a DNA pyramid between AuNPs (~20 nm) and UCNPs ($NaGdF_4$:Yb^{3+}, Er^{3+}, ~19 nm), which carries target-specific sequences enabling a dual-mode detection of miR21 in Hela cells (Figure 5b).[132] The DNA pyramid structure offers a geometric precision to arrange the

DOI: 10.1021/acssensors.8b00257
ACS Sens. 2018, 3, 903−919

chiroptically active AuNPs and luminescent UCNPs with a rational spatial spacer. When this chiral assembly enter cell, target miRNA would hybridize with the recognition domains in DNA structures and disintegrate pyramid integrity. The disassociated nanoparticles could simultaneously induce a chiroplasmonic and a luminescent signal change for dual-mode probing of miRNA in living cells.

DNA nanostructured probes can also specifically recognize the intracellular mRNA transcripts for understanding the state of single cells. Inspired by a natural snail born with a "protective-yet-accessible" biological system, Leong and co-authors devised a TSP-based nanosensor by conjugating a GAPDH mRNA-specific molecular beacon at one vertex, in which the TSP served as nanoshell for protection of beacon within cells (Figure 5c).[133] This noncytotoxic nanosensor is capable of entering living cells without transfection, and highly resistant to nonspecific enzymatic degradation. Upon hybridization with intracellular GAPDH mRNA, the beacon stem-loop structure would unfold and separate the fluorophore from the quencher molecules, thus lighting up the fluorescence signals and mapping the intracellular spatial distribution of target mRNAs. Using this approach, they realized a rapid and highly specific detection of GAPDH mRNA expression in DLD-1 cells at nanomolar sensitivity.

Compared with two-step fabrication of mRNA-responsive TSP, the one-step self-assembly appears more direct and simpler. Tan et al. proposed a single-step DNA tetrahedral nanotweezer that exploited the mRNA-induced fluorescence resonance energy transfer (FRET) for reliable quantification of tumor-related mRNA in living cells (Figure 5d).[134] This nanotweezer contains two fluorescently labeled "arms" respectively positioning on two adjacent vertices, which are partially complementary with different domains of the target mRNA. The initially separated donor and acceptor fluorophores could be brought into close proximity for high-efficiency FRET when precisely tweezing the target mRNA molecule. Such a DNA nanotweezer-based FRET strategy allowed a highly reliable detection of TK1 mRNA in HepG2 cells. To further enhance the detection signal of intracellular TK1 mRNA, Tan et al. used molecular engineering to redesign an entropy-driven tetrahedron-based amplifier that could operate in living cells (Figure 5e).[135] The amplifier operation proceeds through two key molecular modules (i.e., the entropy beacon tetrahedron module and the fuel tetrahedron module) that cooperatively function for signal-enhanced imaging of target mRNA. In the presence of target mRNA, the entropy beacon module can release a beacon complex (turn-off) that has a toehold domain complementary to the fuel module, which fuels the separation of beacon molecules to "turn on" the target-responsive signals. Meanwhile, this process can dehybridize the target mRNA into next round of entropy-driven signal gain. This tetrahedron-based amplifier realized a sensitive detection of TK1 mRNA in HepG2 cells and profiled the expression level of TK1 mRNA in different cell lines.

Apart from these external molecular beacons exposed on the tetrahedral scaffold, an intra-tetrahedral hairpin beacon also serves as an excellent nanoprobe for intracellular mRNA imaging. For example, a specific mRNA-responsive stem-loop structured domain was embedded opposite a nick in one edge of tetrahedron.[136] Without target mRNA, the fluorophore and quencher molecules at each end of the nick were brought into close proximity, which suppressed the fluorescence emission. When this nanoporbe permeates into living HepG2 cells, the target TK1 mRNA specifically hybridizes with the stem-loop structure, thereby inducing a strong fluorescence via target-responsive fluorophore-quencher separation. Despite remarkable progress, such "off-on" tetrahedral nanoprobes often focus one target mRNA. A very recent study demonstrated a simultaneous detection of multiple mRNAs (e.g., C-myc, TK1 and GalNAc-T) in different cell lines, such as MCF-7 and MCF-10A cells (Figure 5f).[137] In this approach, the DNA scaffold harnesses three semiduplex structures (each with a pair of fluorophore-quencher) at different vertices as multicolor-encoded nanoprobes. Upon internalization, the three target mRNAs specifically hybridized with the semiduplex sequences and released the fluorescent strand for intracellular multiple mRNAs detection.

NON-NUCLEIC ACID SENSING

Beyond nucleic acids, there are a variety of living-related signaling substances or physiological microenvironments in cells, ranging from ions, small molecules, proteins to pH and temperature. How to make precise measurement of these important informations is critical for deep understanding of their intracellular spatiotemporal distribution and related functions. To achieve this, several DNA nanostructured probes modified with target-specific functional elements (e.g., aptamer and DNAzyme) have been proposed for accurate probing in living cells. By integrating two metal ion-dependent DNAzyme sequences into two edges of DNA tetrahedron, Xiang et al. developed a dual-color encoded DNA nanoprobe for multiplexed detection of intracellular toxic metal ions.[138] The two ion-specific DNAzyme sequences were respectively embedded into two opposite edges of tetrahedron structure. Each harbors a pair of one fluorophore-two quenchers for effective quenching. Upon recognition with target ions, the specific substrate strands could be sliced by corresponding DNAzymes and thus released the fluorescent fragments for recovering fluorescence. Based on such a dual-color DNAzyme nanoprobe, they realized simultaneous detection of UO_2^{2+} and Pb^{2+} in living HeLa cells (Figure 6a).

Small molecules, such as ATP, can also be sensed in living cells using DNA nanostructured probes. Pei et al. initially incorporated a dynamic ATP-aptamer into one edge of a reconfigurable DNA tetrahedral probe that can serve as an intracellular logic sensor specifically responding to the input of ATP molecules in living HeLa cells.[36] Similarly, a competition strand-mediated DNA tetrahedral probe has also been used to detect intracellular ATP molecules.[139] In this approach, an ATP-aptamer sequence partially hybridizes with its competitor that is a stem-loop structure embedded in one edge of tetrahedral molecular beacon. The presence of target ATP induced a specific ATP-aptamer binding, which gradually recovers the original hairpin structure of the competition strand and initiates FRET signals for ATP readout in living cells (Figure 6b). Different from this independent aptamer probe design, a DNA nanoprism-based split aptamer for ATP was recently used to sense intracellular ATP.[140] Two fragments of the split ATP aptamer were respectively modified with donor and acceptor fluorophores (i.e., Cy3 and Cy5) for FRET, which are partially complementary to the single-stranded edges of DNA triangular prism. Without target, the dual fluorophores are spatially separated at the "FRET off" state, whereas in the presence of target ATP the split aptamer fragment would be brought together, thereby bringing the two fluorophores into close proximity for "FRET on" signaling (Figure 6c). Of note,

DOI: 10.1021/acssensors.8b00257
ACS Sens. 2018, 3, 903−919

DNA nanoprisms, like DNA tetrahedra, are also highly resistant to enzymatic cleavage and have excellent biocompatibility in cells. This nanoprobe combining with split aptamer-based high FRET efficiency allows for effective detection of ATP and probing its intracellular levels in living HeLa cells.

DNA nanostructured probes have also been explored to detect intracellular protein enzymes, such as telomerase, which could catalyze the addition of telomeric repeats. For example, Xu et al. designed an AuNP-based tetrahedral FRET probe for "off−on" fluorescent readout of telomerase activity in cells.[141] A AuNP-conjugated hairpin and three fluorescent dyes (Cy5) are positioned on the four vertices of DNA tetrahedral scaffold. Upon the equal distance between fluorescent dyes and AuNPs on tetrahedron, the self-assembled DNA nanoprobe is initially "FRET-on" due to the strong quench of AuNPs on fluorescent dyes. However, in the presence of telomerase, the stem sequence of hairpin domain could be catalyzed to elongate, which extends the original distance between AuNPs and dyes and thus recovers the fluorescence of Cy5. Using this approach, one telomerase binding event could lighten three reporters, which largely improved the sensitivity of intracellular imaging of telomerase in living HeLa cells (Figure 6d).

In addition to intracellular molecules, DNA nanoprobes are able to read out the intracellular microenvironment, such as pH, superoxide anion ($O_2^{\bullet-}$), and temperature.[142,143] First, Li and coauthors developed DNA tetrahedral probe that is capable of fixing the distance between indicators and enabling simultaneous detection of pH and $O_2^{\bullet-}$ in living cells.[142] This design effectively controls the dye distance and thus avoids the self-quenching of fluorescent dyes, thereby exhibiting much higher sensitivity in imaging as compared to mesoporous silica probes that are prone to suffer from self-quenching. By conjugating one fluorescein (FAM) and three hydroethidine fluorophores on the four vertices, such a signal-enhanced tetrahedral nanoprobe can simultaneously image the dynamic change of pH and $O_2^{\bullet-}$ in living HeLa cells and in vivo at a single wavelength excitation (Figure 6e). Next, a scallop-inspired, thermosensitive DNA nanoprobe was engineered as a nanothermometer to probe intracellular temperature change.[143] This nanoprobe is composed of a DNA tetrahedron with one edge inserted into a thermosensitive molecular beacon (hairpin), which is partially complementary to a dual fluorophore strand (FAM as donor and TAMRA as acceptor) for ratiometric measuring. When the temperature is lower than T_m, the hairpin structure dominates and maintains a contractive DNA nanostructure that brings the donor−acceptor together, whereas at temperature higher than T_m the hairpin unfolds and expands the DNA structure, which would enlarge the distance between donor−acceptor pair (Figure 6f). Using such a reliable FRET-based ratio of acceptor-to-donor fluorescence intensity, a fast and accurate temperature sensing in living cells has been realized.

CONCLUSIONS AND PERSPECTIVES

In this review, we summarize recent progress in FNA-enabled sensing. FNAs can serve as scaffolds for precise engineering of the biosensing interface. We show that FNAs can increase the target accessibility at heterogeneous biosensing interface to improve detection sensitivity and specificity, or enhance the cell permeability without relying on transfection agents. Especially, the precise DNA self-assembly and flexible probe design allow one to modify DNA nanostructures for favorable probe orientation and accessibility at the biosensing interface. Using TSP-based interfacial engineering, various e-TSP and optical sensors have been tailored to measure multiple targets, including ions, small molecules, nucleic acids, antibodies, exosomes and cancer cells.[144] FNAs have also been exploited to use as functional "liquid chips" or carrier platforms, which harness the synergistic effect of probe anchoring with atomic precision and homogeneous molecular recognition for highly sensitive detection of target substances. In combination with their prominent properties, such as endocytotic internalization, enzymatic resistance, and noncytotoxicity,[128,145,146] FNAs can effectively transduce the intracellular molecular events or monitor the microenvironments in living cells.

Despite the remarkable progress, there are still several challenges in FNA-enabled sensing. (i) The purity of self-assembled DNA nanostructures governs their downstream application, including biosensing. Nevertheless, the purification means currently is limited by gel electrophoresis, chromatography, and centrifugation techniques.[147−149] This requires that approaches with higher separation efficiency, for example, single-step rapid isolation, to be developed.[150] (ii) Solid-phase synthesis of long DNA sequences (>100 nt) remains a hurdle. Besides, DNA nanostructures, such as origami, often require hundreds of staple ssDNA to complete structural folding. Both would contribute to high cost in building functional DNA nanostructures.[151] Very recently, Dietz et al. reported a cost-effective and scalable approach capable of producing ssDNA with virtually arbitrary sequence and length.[24] In this approach, they used bacteriophages to derive target sequence-contained ssDNA precursor that interleave with Zn^{2+}-dependent self-excising DNAzyme cassettes for mass production of the ssDNA required in DNA origami. (iii) DNA nanostructures can carry cargo into cytoplasm inside living cells, while their organelle targetability remains to be improved. This largely hinders the roles of FNAs in deciphering intracellular molecular events. We believe that the rapid evolution and interdisciplinarity of DNA nanotechnology would create more FNAs to enable precise molecular handling and biosensing.[7,152−155]

We expect that synthetic biology, conjugation techniques, and smart bioresponsive materials might be exploited to tailor FNAs for better interfacial orientation or more flexible responsiveness for in vitro detection.[6,156−160] By taking TSP-antibody or TSP-aptamer complex as an example, it has a synergistic structural advantage that contributes to either a renewable probe layer, favorable accessibility at an interface, or a powerful intracellular molecular beacon.[27,106,144] Note that the nanoscale structure usually accelerates the mass transport rate and improves the sensitivity.[85] However, the limited space available in nanosensors restricts the effective probe numbers and biorecognition events. To address this size dilemma, a trans-scale biosensor that incorporates nanoarchitectures into macroscopic surfaces is highly desirable.[48,161,162] For example, by patterning the macroscopic gold electrode with TSP varying in size, the detection limit can be programmably tuned.[48] These artificial DNA nanoprobes may also be modulated by electric fields to enhance the biorecognition capacity.[163,164] By interfacing with a single-step, multiplexed microfluidic system, the functional structured bioprobes would be promising to enable precise quantification of clinically relevant markers at different levels.[125,165,166] We envision that FNAs will provide numerous opportunities for a new generation of molecular diagnosis and therapy.[167−171]

DOI: 10.1021/acssensors.8b00257
ACS Sens. 2018, 3, 903−919

AUTHOR INFORMATION

Corresponding Authors

*E-mail: fchh@sinap.ac.cn.
*E-mail: gjzhangtj@hotmail.com.

ORCID

Fan Yang: 0000-0002-8490-4183
Qian Li: 0000-0002-1166-6583
Lihua Wang: 0000-0002-6198-7561
Guo-Jun Zhang: 0000-0001-9096-9226
Chunhai Fan: 0000-0002-7171-7338

Notes

The authors declare no competing financial interest.

ACKNOWLEDGMENTS

The authors are thankful for the support for part of the work described in this review, which includes the Ministry of Science and Technology of China (2016YFA0201200, 2016YFA0400900, 2015CB559100, and 2016YFC0903402), the National Natural Science Foundation of China (21775034, 21675167, and 21675041), the National Science Foundation for Distinguished Young Scholars of Hubei Province (2018CFA041), Hubei Province health and family planning scientific research project (WJ2017Q032), and the Key Research Program of Frontier Sciences (QYZDJ-SSW-SLH031), the Open Large Infrastructure Research of CAS, Chinese Academy of Sciences.

VOCABULARY

Framework nucleic acids, exquisite DNA or RNA nanostructures assembled through highly predictable and precise DNA hybridization, which provide frameworks for organizing molecules or materials; structural DNA nanotechnology, a DNA-based technology using precise Watson−Crick base-pairing rules to construct DNA nanostructures from 1D to 3D with high controllability and programmability; tetrahedral structured probe, a tetrahedron-shaped scaffold assembled with designed DNA sequences for precisely anchoring of biomolecular probes; interface engineering, using engineering principles to design and modulate interface properties; intracellular biosensing, translate biological recognition events inside cells into measurable physical signals

REFERENCES

(1) Seeman, N. C. DNA in a material world. *Nature* **2003**, *421* (6921), 427−431.
(2) Seeman, N. C. Nanomaterials Based on DNA. *Annu. Rev. Biochem.* **2010**, *79* (1), 65−87.
(3) Aldaye, F. A.; Palmer, A. L.; Sleiman, H. F. Assembling materials with DNA as the guide. *Science* **2008**, *321* (5897), 1795−1799.
(4) Jones, M. R.; Seeman, N. C.; Mirkin, C. A. Programmable materials and the nature of the DNA bond. *Science* **2015**, *347* (6224), 1260901.
(5) Wang, Z.-G.; Ding, B. Engineering DNA Self-Assemblies as Templates for Functional Nanostructures. *Acc. Chem. Res.* **2014**, *47* (6), 1654−1662.
(6) Li, J.; Green, A. A.; Yan, H.; Fan, C. Engineering nucleic acid structures for programmable molecular circuitry and intracellular biocomputation. *Nat. Chem.* **2017**, *9*, 1056.
(7) Seeman, N. C.; Sleiman, H. F. DNA nanotechnology. *Nat. Rev. Mater.* **2017**, *3*, 17068.
(8) He, Y.; Chen, Y.; Liu, H.; Ribbe, A. E.; Mao, C. Self-assembly of hexagonal DNA two-dimensional (2D) arrays. *J. Am. Chem. Soc.* **2005**, *127* (35), 12202−12203.
(9) Qian, L.; Wang, Y.; Zhang, Z.; Zhao, J.; Pan, D.; Zhang, Y.; Liu, Q.; Fan, C.; Hu, J.; He, L. Analogic China map constructed by DNA. *Chin. Sci. Bull.* **2006**, *51* (24), 2973−2976.
(10) Xing, Y.; Yang, Z.; Liu, D. A Responsive Hidden Toehold To Enable Controllable DNA Strand Displacement Reactions. *Angew. Chem., Int. Ed.* **2011**, *50* (50), 11934−11936.
(11) Douglas, S. M.; Dietz, H.; Liedl, T.; Högberg, B.; Graf, F.; Shih, W. M. Self-assembly of DNA into nanoscale three-dimensional shapes. *Nature* **2009**, *459*, 414.
(12) Liedl, T.; Högberg, B.; Tytell, J.; Ingber, D. E.; Shih, W. M. Self-assembly of three-dimensional prestressed tensegrity structures from DNA. *Nat. Nanotechnol.* **2010**, *5*, 520.
(13) Han, D.; Pal, S.; Liu, Y.; Yan, H. Folding and cutting DNA into reconfigurable topological nanostructures. *Nat. Nanotechnol.* **2010**, *5*, 712.
(14) Ke, Y.; Ong, L. L.; Shih, W. M.; Yin, P. Three-Dimensional Structures Self-Assembled from DNA Bricks. *Science* **2012**, *338* (6111), 1177−1183.
(15) Wei, B.; Dai, M.; Yin, P. Complex shapes self-assembled from single-stranded DNA tiles. *Nature* **2012**, *485*, 623.
(16) Hong, F.; Zhang, F.; Liu, Y.; Yan, H. DNA Origami: Scaffolds for Creating Higher Order Structures. *Chem. Rev.* **2017**, *117* (20), 12584−12640.
(17) He, Y.; Tian, Y.; Chen, Y.; Deng, Z.; Ribbe, A. E.; Mao, C. Sequence symmetry as a tool for designing DNA nanostructures. *Angew. Chem.* **2005**, *117* (41), 6852−6854.
(18) He, Y.; Ye, T.; Su, M.; Zhang, C.; Ribbe, A. E.; Jiang, W.; Mao, C. Hierarchical self-assembly of DNA into symmetric supramolecular polyhedra. *Nature* **2008**, *452* (7184), 198.
(19) Andersen, E. S.; Dong, M.; Nielsen, M. M.; Jahn, K.; Subramani, R.; Mamdouh, W.; Golas, M. M.; Sander, B.; Stark, H.; Oliveira, C. L. P.; Pedersen, J. S.; Birkedal, V.; Besenbacher, F.; Gothelf, K. V.; Kjems, J. Self-assembly of a nanoscale DNA box with a controllable lid. *Nature* **2009**, *459*, 73.
(20) Han, D.; Pal, S.; Nangreave, J.; Deng, Z.; Liu, Y.; Yan, H. DNA Origami with Complex Curvatures in Three-Dimensional Space. *Science* **2011**, *332* (6027), 342−346.
(21) Tikhomirov, G.; Petersen, P.; Qian, L. Fractal assembly of micrometre-scale DNA origami arrays with arbitrary patterns. *Nature* **2017**, *552*, 67.
(22) Wagenbauer, K. F.; Sigl, C.; Dietz, H. Gigadalton-scale shape-programmable DNA assemblies. *Nature* **2017**, *552*, 78.
(23) Ong, L. L.; Hanikel, N.; Yaghi, O. K.; Grun, C.; Strauss, M. T.; Bron, P.; Lai-Kee-Him, J.; Schueder, F.; Wang, B.; Wang, P.; Kishi, J. Y.; Myhrvold, C.; Zhu, A.; Jungmann, R.; Bellot, G.; Ke, Y.; Yin, P. Programmable self-assembly of three-dimensional nanostructures from 10,000 unique components. *Nature* **2017**, *552*, 72.
(24) Praetorius, F.; Kick, B.; Behler, K. L.; Honemann, M. N.; Weuster-Botz, D.; Dietz, H. Biotechnological mass production of DNA origami. *Nature* **2017**, *552*, 84.
(25) Lin, M.; Song, P.; Zhou, G.; Zuo, X.; Aldalbahi, A.; Lou, X.; Shi, J.; Fan, C. Electrochemical detection of nucleic acids, proteins, small molecules and cells using a DNA-nanostructure-based universal biosensing platform. *Nat. Protoc.* **2016**, *11* (7), 1244−1263.
(26) Ye, D.; Zuo, X.; Fan, C. DNA nanostructure-based engineering of the biosensing interface for biomolecular detection. *Prog. Chem.* **2017**, *29* (1), 36−46.
(27) Xie, N.; Liu, S.; Yang, X.; He, X.; Huang, J.; Wang, K. DNA tetrahedron nanostructures for biological applications: biosensors and drug delivery. *Analyst* **2017**, *142* (18), 3322−3332.
(28) Hu, Y.; Chen, Z.; Zhang, H.; Li, M.; Hou, Z.; Luo, X.; Xue, X. Development of DNA tetrahedron-based drug delivery system. *Drug Delivery* **2017**, *24* (1), 1295−1301.
(29) Ouyang, X.; Li, J.; Liu, H.; Zhao, B.; Yan, J.; Ma, Y.; Xiao, S.; Song, S.; Huang, Q.; Chao, J.; Fan, C. Rolling Circle Amplification-Based DNA Origami Nanostructrures for Intracellular Delivery of Immunostimulatory Drugs. *Small* **2013**, *9* (18), 3082−3087.
(30) Zhang, Y.; Tu, J.; Wang, D.; Zhu, H.; Maity, S. K.; Qu, X.; Bogaert, B.; Pei, H.; Zhang, H. Programmable and Multifunctional

DOI: 10.1021/acssensors.8b00257
ACS Sens. 2018, 3, 903−919

DNA-Based Materials for Biomedical Applications. *Adv. Mater.* **2018**, 1703658.
(31) Lu, C.-H.; Willner, B.; Willner, I. DNA nanotechnology: from sensing and DNA machines to drug-delivery systems. *ACS Nano* **2013**, *7* (10), 8320−8332.
(32) Mao, C.; Sun, W.; Seeman, N. C. Designed Two-Dimensional DNA Holliday Junction Arrays Visualized by Atomic Force Microscopy. *J. Am. Chem. Soc.* **1999**, *121* (23), 5437−5443.
(33) Kolpashchikov, D. M. A Binary DNA Probe for Highly Specific Nucleic Acid Recognition. *J. Am. Chem. Soc.* **2006**, *128* (32), 10625−10628.
(34) Goodman, R. P.; Berry, R. M.; Turberfield, A. J. The single-step synthesis of a DNA tetrahedron. *Chem. Commun.* **2004**, *12*, 1372−1373.
(35) Pei, H.; Lu, N.; Wen, Y.; Song, S.; Liu, Y.; Yan, H.; Fan, C. A DNA Nanostructure-based Biomolecular Probe Carrier Platform for Electrochemical Biosensing. *Adv. Mater.* **2010**, *22* (42), 4754−4758.
(36) Pei, H.; Liang, L.; Yao, G.; Li, J.; Huang, Q.; Fan, C. Reconfigurable three-dimensional DNA nanostructures for the construction of intracellular logic sensors. *Angew. Chem.* **2012**, *124* (36), 9154−9158.
(37) Rothemund, P. W. Folding DNA to create nanoscale shapes and patterns. *Nature* **2006**, *440* (7082), 297.
(38) Um, S. H.; Lee, J. B.; Park, N.; Kwon, S. Y.; Umbach, C. C.; Luo, D. Enzyme-catalysed assembly of DNA hydrogel. *Nat. Mater.* **2006**, *5*, 797.
(39) Ke, Y.; Lindsay, S.; Chang, Y.; Liu, Y.; Yan, H. Self-assembled water-soluble nucleic acid probe tiles for label-free RNA hybridization assays. *Science* **2008**, *319* (5860), 180−183.
(40) Wang, D.; Hu, Y.; Liu, P.; Luo, D. Bioresponsive DNA Hydrogels: Beyond the Conventional Stimuli Responsiveness. *Acc. Chem. Res.* **2017**, *50* (4), 733−739.
(41) Bell, N. A. W.; Engst, C. R.; Ablay, M.; Divitini, G.; Ducati, C.; Liedl, T.; Keyser, U. F. DNA Origami Nanopores. *Nano Lett.* **2012**, *12* (1), 512−517.
(42) Hemmig, E. A.; Fitzgerald, C.; Maffeo, C.; Hecker, L.; Ochmann, S. E.; Aksimentiev, A.; Tinnefeld, P.; Keyser, U. F. Optical Voltage Sensing Using DNA Origami. *Nano Lett.* **2018**, *18* (3), 1962−1971.
(43) Edwardson, T. G. W.; Carneiro, K. M. M.; McLaughlin, C. K.; Serpell, C. J.; Sleiman, H. F. Site-specific positioning of dendritic alkyl chains on DNA cages enables their geometry-dependent self-assembly. *Nat. Chem.* **2013**, *5*, 868.
(44) Conway, J. W.; Madwar, C.; Edwardson, T. G.; McLaughlin, C. K.; Fahkoury, J.; Lennox, R. B.; Sleiman, H. F. Dynamic Behavior of DNA Cages Anchored on Spherically Supported Lipid Bilayers. *J. Am. Chem. Soc.* **2014**, *136* (37), 12987−12997.
(45) Edwardson, T. G. W.; Lau, K. L.; Bousmail, D.; Serpell, C. J.; Sleiman, H. F. Transfer of molecular recognition information from DNA nanostructures to gold nanoparticles. *Nat. Chem.* **2016**, *8*, 162.
(46) Zhang, Y.; Chao, J.; Liu, H.; Wang, F.; Su, S.; Liu, B.; Zhang, L.; Shi, J.; Wang, L.; Huang, W.; Wang, L.; Fan, C. Transfer of Two-Dimensional Oligonucleotide Patterns onto Stereocontrolled Plasmonic Nanostructures through DNA-Origami-Based Nanoimprinting Lithography. *Angew. Chem., Int. Ed.* **2016**, *55* (28), 8036−8040.
(47) Chao, J.; Zhang, Y.; Zhu, D.; Liu, B.; Cui, C.; Su, S.; Fan, C.; Wang, L. Hetero-assembly of gold nanoparticles on a DNA origami template. *Sci. China: Chem.* **2016**, *59* (6), 730−734.
(48) Lin, M.; Wang, J.; Zhou, G.; Wang, J.; Wu, N.; Lu, J.; Gao, J.; Chen, X.; Shi, J.; Zuo, X.; Fan, C. Programmable Engineering of a Biosensing Interface with Tetrahedral DNA Nanostructures for Ultrasensitive DNA Detection. *Angew. Chem., Int. Ed.* **2015**, *54* (7), 2151−2155.
(49) Li, J.; Pei, H.; Zhu, B.; Liang, L.; Wei, M.; He, Y.; Chen, N.; Li, D.; Huang, Q.; Fan, C. Self-assembled multivalent DNA nanostructures for noninvasive intracellular delivery of immunostimulatory CpG oligonucleotides. *ACS Nano* **2011**, *5* (11), 8783−8789.
(50) Chao, J.; Zhu, D.; Zhang, Y.; Wang, L.; Fan, C. DNA nanotechnology-enabled biosensors. *Biosens. Bioelectron.* **2016**, *76*, 68−79.
(51) Zhang, H.-Z.; Zhang, Z.-Q.; Wang, F.; Zhou, T.; Wang, X.-F.; Zhang, G.-D.; Liu, T.-T.; Liu, S.-Z. Application of Structural DNA Nanotechnology. *Acta Phys.-Chim. Sin.* **2017**, *33* (8), 1520−1532.
(52) Zhou, X.; Zhao, M.; Duan, X.; Guo, B.; Cheng, W.; Ding, S.; Ju, H. Collapse of DNA Tetrahedron Nanostructure for "Off−On" Fluorescence Detection of DNA Methyltransferase Activity. *ACS Appl. Mater. Interfaces* **2017**, *9* (46), 40087−40093.
(53) Yang, X.; Wen, Y.; Wang, L.; Zhou, C.; Li, Q.; Xu, L.; Li, L.; Shi, J.; Lal, R.; Ren, S.; Li, J.; Jia, N.; Liu, G. PCR-Free Colorimetric DNA Hybridization Detection Using a 3D DNA Nanostructured Reporter Probe. *ACS Appl. Mater. Interfaces* **2017**, *9* (44), 38281−38287.
(54) Xu, F.; Dong, H.; Cao, Y.; Lu, H.; Meng, X.; Dai, W.; Zhang, X.; Al-Ghanim, K. A.; Mahboob, S. Ultrasensitive and Multiple Disease-Related MicroRNA Detection Based on Tetrahedral DNA Nanostructures and Duplex-Specific Nuclease-Assisted Signal Amplification. *ACS Appl. Mater. Interfaces* **2016**, *8* (49), 33499−33505.
(55) Gu, H.; Chao, J.; Xiao, S.-J.; Seeman, N. C. Dynamic patterning programmed by DNA tiles captured on a DNA origami substrate. *Nat. Nanotechnol.* **2009**, *4*, 245.
(56) Kolpashchikov, D. M.; Gerasimova, Y. V.; Khan, M. S. DNA Nanotechnology for Nucleic Acid Analysis: DX Motif-Based Sensor. *ChemBioChem* **2011**, *12* (17), 2564−2567.
(57) Zhang, Z.; Wang, Y.; Fan, C.; Li, C.; Li, Y.; Qian, L.; Fu, Y.; Shi, Y.; Hu, J.; He, L. Asymmetric DNA Origami for Spatially Addressable and Index-Free Solution-Phase DNA Chips. *Adv. Mater.* **2010**, *22* (24), 2672−2675.
(58) Zhang, Z.; Zeng, D.; Ma, H.; Feng, G.; Hu, J.; He, L.; Li, C.; Fan, C. A DNA-Origami Chip Platform for Label-Free SNP Genotyping Using Toehold-Mediated Strand Displacement. *Small* **2010**, *6* (17), 1854−1858.
(59) Subramanian, H. K.; Chakraborty, B.; Sha, R.; Seeman, N. C. The label-free unambiguous detection and symbolic display of single nucleotide polymorphisms on DNA origami. *Nano Lett.* **2011**, *11* (2), 910−913.
(60) Wang, D.; Fu, Y.; Yan, J.; Zhao, B.; Dai, B.; Chao, J.; Liu, H.; He, D.; Zhang, Y.; Fan, C.; Song, S. Molecular Logic Gates on DNA Origami Nanostructures for MicroRNA Diagnostics. *Anal. Chem.* **2014**, *86* (4), 1932−1936.
(61) Zhang, H.; Chao, J.; Pan, D.; Liu, H.; Qiang, Y.; Liu, K.; Cui, C.; Chen, J.; Huang, Q.; Hu, J.; Wang, L.; Huang, W.; Shi, Y.; Fan, C. DNA origami-based shape IDs for single-molecule nanomechanical genotyping. *Nat. Commun.* **2017**, *8*, 14738.
(62) Liu, K.; Pan, D.; Wen, Y.; Zhang, H.; Chao, J.; Wang, L.; Song, S.; Fan, C.; Shi, Y. Identifying the Genotypes of Hepatitis B Virus (HBV) with DNA Origami Label. *Small* **2018**, *14* (6), 1701718.
(63) Fu, J.; Yang, Y. R.; Dhakal, S.; Zhao, Z.; Liu, M.; Zhang, T.; Walter, N. G.; Yan, H. Assembly of multienzyme complexes on DNA nanostructures. *Nat. Protoc.* **2016**, *11*, 2243.
(64) Fu, J.; Liu, M.; Liu, Y.; Woodbury, N. W.; Yan, H. Interenzyme substrate diffusion for an enzyme cascade organized on spatially addressable DNA nanostructures. *J. Am. Chem. Soc.* **2012**, *134* (12), 5516−5519.
(65) Fu, Y.; Zeng, D.; Chao, J.; Jin, Y.; Zhang, Z.; Liu, H.; Li, D.; Ma, H.; Huang, Q.; Gothelf, K. V.; Fan, C. Single-step rapid assembly of DNA origami nanostructures for addressable nanoscale bioreactors. *J. Am. Chem. Soc.* **2013**, *135* (2), 696−702.
(66) Zhao, Z.; Fu, J.; Dhakal, S.; Johnson-Buck, A.; Liu, M.; Zhang, T.; Woodbury, N. W.; Liu, Y.; Walter, N. G.; Yan, H. Nanocaged enzymes with enhanced catalytic activity and increased stability against protease digestion. *Nat. Commun.* **2016**, *7*, 10619.
(67) Yan, J.; Hu, C.; Wang, P.; Liu, R.; Zuo, X.; Liu, X.; Song, S.; Fan, C.; He, D.; Sun, G. Novel rolling circle amplification and DNA origami-based DNA belt-involved signal amplification assay for highly sensitive detection of prostate-specific antigen (PSA). *ACS Appl. Mater. Interfaces* **2014**, *6* (22), 20372−20377.

DOI: 10.1021/acssensors.8b00257
ACS Sens. 2018, 3, 903−919

(68) Bell, N. A. W.; Keyser, U. F. Nanopores formed by DNA origami: A review. *FEBS Lett.* **2014**, *588* (19), 3564−3570.
(69) Cao, C.; Ying, Y.-L.; Hu, Z.-L.; Liao, D.-F.; Tian, H.; Long, Y.-T. Discrimination of oligonucleotides of different lengths with a wild-type aerolysin nanopore. *Nat. Nanotechnol.* **2016**, *11*, 713.
(70) Hall, A. R.; Scott, A.; Rotem, D.; Mehta, K. K.; Bayley, H.; Dekker, C. Hybrid pore formation by directed insertion of α-haemolysin into solid-state nanopores. *Nat. Nanotechnol.* **2010**, *5*, 874.
(71) Hernández-Ainsa, S.; Bell, N. A. W.; Thacker, V. V.; Göpfrich, K.; Misiunas, K.; Fuentes-Perez, M. E.; Moreno-Herrero, F.; Keyser, U. F. DNA Origami Nanopores for Controlling DNA Translocation. *ACS Nano* **2013**, *7* (7), 6024−6030.
(72) Wei, R.; Martin, T. G.; Rant, U.; Dietz, H. DNA Origami Gatekeepers for Solid-State Nanopores. *Angew. Chem., Int. Ed.* **2012**, *51* (20), 4864−4867.
(73) Langecker, M.; Arnaut, V.; Martin, T. G.; List, J.; Renner, S.; Mayer, M.; Dietz, H.; Simmel, F. C. Synthetic Lipid Membrane Channels Formed by Designed DNA Nanostructures. *Science* **2012**, *338* (6109), 932−936.
(74) Krishnan, S.; Ziegler, D.; Arnaut, V.; Martin, T. G.; Kapsner, K.; Henneberg, K.; Bausch, A. R.; Dietz, H.; Simmel, F. C. Molecular transport through large-diameter DNA nanopores. *Nat. Commun.* **2016**, *7*, 12787.
(75) Barati Farimani, A.; Dibaeinia, P.; Aluru, N. R. DNA Origami−Graphene Hybrid Nanopore for DNA Detection. *ACS Appl. Mater. Interfaces* **2017**, *9* (1), 92−100.
(76) Kahn, J. S.; Hu, Y.; Willner, I. Stimuli-Responsive DNA-Based Hydrogels: From Basic Principles to Applications. *Acc. Chem. Res.* **2017**, *50* (4), 680−690.
(77) Culver, H. R.; Clegg, J. R.; Peppas, N. A. Analyte-Responsive Hydrogels: Intelligent Materials for Biosensing and Drug Delivery. *Acc. Chem. Res.* **2017**, *50* (2), 170−178.
(78) Shao, Y.; Jia, H.; Cao, T.; Liu, D. Supramolecular Hydrogels Based on DNA Self-Assembly. *Acc. Chem. Res.* **2017**, *50* (4), 659−668.
(79) Wang, J.; Chao, J.; Liu, H.; Su, S.; Wang, L.; Huang, W.; Willner, I.; Fan, C. Clamped Hybridization Chain Reactions for the Self-Assembly of Patterned DNA Hydrogels. *Angew. Chem., Int. Ed.* **2017**, *56* (8), 2171−2175.
(80) Lee, J. B.; Peng, S.; Yang, D.; Roh, Y. H.; Funabashi, H.; Park, N.; Rice, E. J.; Chen, L.; Long, R.; Wu, M.; Luo, D. A mechanical metamaterial made from a DNA hydrogel. *Nat. Nanotechnol.* **2012**, *7* (12), 816.
(81) Zhang, L.; Lei, J.; Liu, L.; Li, C.; Ju, H. Self-assembled DNA hydrogel as switchable material for aptamer-based fluorescent detection of protein. *Anal. Chem.* **2013**, *85* (22), 11077−11082.
(82) Song, P.; Ye, D.; Zuo, X.; Li, J.; Wang, J.; Liu, H.; Hwang, M. T.; Chao, J.; Su, S.; Wang, L.; Shi, J.; Wang, L.; Huang, W.; Lal, R.; Fan, C. DNA Hydrogel with Aptamer-Toehold-Based Recognition, Cloaking, and Decloaking of Circulating Tumor Cells for Live Cell Analysis. *Nano Lett.* **2017**, *17* (9), 5193−5198.
(83) Zhong, R.; Tang, Q.; Wang, S.; Zhang, H.; Zhang, F.; Xiao, M.; Man, T.; Qu, X.; Li, L.; Zhang, W.; Pei, H. Self-Assembly of Enzyme-Like Nanofibrous G-Molecular Hydrogel for Printed Flexible Electrochemical Sensors. *Adv. Mater.* **2018**, *30*, 1706887.
(84) Zhong, R.; Xiao, M.; Zhu, C.; Shen, X.; Tang, Q.; Zhang, W.; Wang, L.; Song, S.; Qu, X.; Pei, H.; Wang, C.; Li, L. Logic Catalytic Interconversion of G-Molecular Hydrogel. *ACS Appl. Mater. Interfaces* **2018**, *10* (5), 4512−4518.
(85) Squires, T. M.; Messinger, R. J.; Manalis, S. R. Making it stick: convection, reaction and diffusion in surface-based biosensors. *Nat. Biotechnol.* **2008**, *26* (4), 417−426.
(86) Mitchell, N.; Schlapak, R.; Kastner, M.; Armitage, D.; Chrzanowski, W.; Riener, J.; Hinterdorfer, P.; Ebner, A.; Howorka, S. A DNA Nanostructure for the Functional Assembly of Chemical Groups with Tunable Stoichiometry and Defined Nanoscale Geometry. *Angew. Chem., Int. Ed.* **2009**, *48* (3), 525−527.
(87) Pei, H.; Zuo, X.; Pan, D.; Shi, J.; Huang, Q.; Fan, C. Scaffolded biosensors with designed DNA nanostructures. *NPG Asia Mater.* **2013**, *5*, e51.
(88) Dong, S.; Zhao, R.; Zhu, J.; Lu, X.; Li, Y.; Qiu, S.; Jia, L.; Jiao, X.; Song, S.; Fan, C.; Hao, R.; Song, H. Electrochemical DNA Biosensor Based on a Tetrahedral Nanostructure Probe for the Detection of Avian Influenza A (H7N9) Virus. *ACS Appl. Mater. Interfaces* **2015**, *7* (16), 8834−8842.
(89) Wen, Y.; Wang, L.; Xu, L.; Li, L.; Ren, S.; Cao, C.; Jia, N.; Aldalbahi, A.; Song, S.; Shi, J.; et al. Electrochemical detection of PCR amplicons of Escherichia coli genome based on DNA nanostructural probes and polyHRP enzyme. *Analyst* **2016**, *141* (18), 5304−5310.
(90) Ge, Z.; Lin, M.; Wang, P.; Pei, H.; Yan, J.; Shi, J.; Huang, Q.; He, D.; Fan, C.; Zuo, X. Hybridization Chain Reaction Amplification of MicroRNA Detection with a Tetrahedral DNA Nanostructure-Based Electrochemical Biosensor. *Anal. Chem.* **2014**, *86* (4), 2124−2130.
(91) Wang, X.; Chen, F.; Zhang, D.; Zhao, Y.; Wei, J.; Wang, L.; Song, S.; Fan, C.; Zhao, Y. Single copy-sensitive electrochemical assay for circulating methylated DNA in clinical samples with ultrahigh specificity based on a sequential discrimination-amplification strategy. *Chem. Sci.* **2017**, *8* (7), 4764−4770.
(92) Ge, Z.; Pei, H.; Wang, L.; Song, S.; Fan, C. Electrochemical single nucleotide polymorphisms genotyping on surface immobilized three-dimensional branched DNA nanostructure. *Sci. China: Chem.* **2011**, *54* (8), 1273.
(93) Li, Z.; Su, W.; Liu, S.; Ding, X. An electrochemical biosensor based on DNA tetrahedron/graphene composite film for highly sensitive detection of NADH. *Biosens. Bioelectron.* **2015**, *69*, 287−293.
(94) Li, Y.; Wen, Y.; Wang, L.; Liang, W.; Xu, L.; Ren, S.; Zou, Z.; Zuo, X.; Fan, C.; Huang, Q.; Liu, G.; Jia, N. Analysis of telomerase activity based on a spired DNA tetrahedron TS primer. *Biosens. Bioelectron.* **2015**, *67*, 364−369.
(95) Fan, J.; Liu, Y.; Xu, E.; Zhang, Y.; Wei, W.; Yin, L.; Pu, Y.; Liu, S. A label-free ultrasensitive assay of 8-hydroxy-2′-deoxyguanosine in human serum and urine samples via polyaniline deposition and tetrahedral DNA nanostructure. *Anal. Chim. Acta* **2016**, *946*, 48−55.
(96) Feng, Q.-M.; Zhou, Z.; Li, M.-X.; Zhao, W.; Xu, J.-J.; Chen, H.-Y. DNA tetrahedral scaffolds-based platform for the construction of electrochemiluminescence biosensor. *Biosens. Bioelectron.* **2017**, *90*, 251−257.
(97) Wen, Y.; Liu, G.; Pei, H.; Li, L.; Xu, Q.; Liang, W.; Li, Y.; Xu, L.; Ren, S.; Fan, C. DNA nanostructure-based ultrasensitive electrochemical microRNA biosensor. *Methods* **2013**, *64* (3), 276−282.
(98) Huang, Y. L.; Mo, S.; Gao, Z. F.; Chen, J. R.; Lei, J. L.; Luo, H. Q.; Li, N. B. Amperometric biosensor for microRNA based on the use of tetrahedral DNA nanostructure probes and guanine nanowire amplification. *Microchim. Acta* **2017**, *184* (8), 2597−2604.
(99) Lin, M.; Wen, Y.; Li, L.; Pei, H.; Liu, G.; Song, H.; Zuo, X.; Fan, C.; Huang, Q. Target-Responsive, DNA Nanostructure-Based E-DNA Sensor for microRNA Analysis. *Anal. Chem.* **2014**, *86* (5), 2285−2288.
(100) Wen, Y.; Pei, H.; Shen, Y.; Xi, J.; Lin, M.; Lu, N.; Shen, X.; Li, J.; Fan, C. DNA Nanostructure-based Interfacial engineering for PCR-free ultrasensitive electrochemical analysis of microRNA. *Sci. Rep.* **2012**, *2*, 867.
(101) Liu, S.-Z.; Zhang, Z.-Q.; Wang, F.; Zhou, T.; Wang, X.-F.; Zhang, G.-D.; Liu, T.-T.; Zhang, H.-Z. Study on the Synthesis of DNA via Rolling Circle Amplification. *Acta Phys.-Chim. Sin.* **2017**, *33* (10), 2052−2057.
(102) Miao, P.; Tang, Y.; Yin, J. MicroRNA detection based on analyte triggered nanoparticle localization on a tetrahedral DNA modified electrode followed by hybridization chain reaction dual amplification. *Chem. Commun.* **2015**, *51* (86), 15629−15632.
(103) Miao, P.; Wang, B.; Chen, X.; Li, X.; Tang, Y. Tetrahedral DNA Nanostructure-Based MicroRNA Biosensor Coupled with Catalytic Recycling of the Analyte. *ACS Appl. Mater. Interfaces* **2015**, *7* (11), 6238−6243.
(104) Miao, P.; Wang, B.; Meng, F.; Yin, J.; Tang, Y. Ultrasensitive Detection of MicroRNA through Rolling Circle Amplification on a DNA Tetrahedron Decorated Electrode. *Bioconjugate Chem.* **2015**, *26* (3), 602−607.

DOI: 10.1021/acssensors.8b00257
ACS Sens. 2018, 3, 903−919

(105) Zeng, D.; Wang, Z.; Meng, Z.; Wang, P.; San, L.; Wang, W.; Aldalbahi, A.; Li, L.; Shen, J.; Mi, X. DNA tetrahedral nanostructure-based electrochemical miRNA biosensor for simultaneous detection of multiple miRNAs in pancreatic carcinoma. *ACS Appl. Mater. Interfaces* **2017**, *9* (28), 24118−24125.
(106) Pei, H.; Wan, Y.; Li, J.; Hu, H.; Su, Y.; Huang, Q.; Fan, C. Regenerable electrochemical immunological sensing at DNA nanostructure-decorated gold surfaces. *Chem. Commun.* **2011**, *47* (22), 6254−6256.
(107) Chen, X.; Zhou, G.; Song, P.; Wang, J.; Gao, J.; Lu, J.; Fan, C.; Zuo, X. Ultrasensitive Electrochemical Detection of Prostate-Specific Antigen by Using Antibodies Anchored on a DNA Nanostructural Scaffold. *Anal. Chem.* **2014**, *86* (15), 7337−7342.
(108) Yuan, L.; Giovanni, M.; Xie, J.; Fan, C.; Leong, D. T. Ultrasensitive IgG quantification using DNA nano-pyramids. *NPG Asia Mater.* **2014**, *6*, e112.
(109) Giovanni, M.; Setyawati, M. I.; Tay, C. Y.; Qian, H.; Kuan, W. S.; Leong, D. T. Electrochemical quantification of Escherichia coli with DNA nanostructure. *Adv. Funct. Mater.* **2015**, *25* (25), 3840−3846.
(110) Wang, J.; Leong, M. C.; Leong, E. Z. W.; Kuan, W. S.; Leong, D. T. Clinically Relevant Detection of Streptococcus pneumoniae with DNA-Antibody Nanostructures. *Anal. Chem.* **2017**, *89* (12), 6900−6906.
(111) Wen, Y.; Pei, H.; Wan, Y.; Su, Y.; Huang, Q.; Song, S.; Fan, C. DNA Nanostructure-Decorated Surfaces for Enhanced Aptamer-Target Binding and Electrochemical Cocaine Sensors. *Anal. Chem.* **2011**, *83* (19), 7418−7423.
(112) Bu, N.-N.; Gao, A.; He, X.-W.; Yin, X.-B. Electrochemiluminescent biosensor of ATP using tetrahedron structured DNA and a functional oligonucleotide for Ru(phen)3 2+ intercalation and target identification. *Biosens. Bioelectron.* **2013**, *43*, 200−204.
(113) Bu, N.-N.; Tang, C.-X.; He, X.-W.; Yin, X.-B. Tetrahedron-structured DNA and functional oligonucleotide for construction of an electrochemical DNA-based biosensor. *Chem. Commun.* **2011**, *47* (27), 7689−7691.
(114) Li, C.; Hu, X.; Lu, J.; Mao, X.; Xiang, Y.; Shu, Y.; Li, G. Design of DNA nanostructure-based interfacial probes for the electrochemical detection of nucleic acids directly in whole blood. *Chem. Sci.* **2018**, *9*, 979−984.
(115) Wang, S.; Zhang, L.; Wan, S.; Cansiz, S.; Cui, C.; Liu, Y.; Cai, R.; Hong, C.; Teng, I. T.; Shi, M.; Wu, Y.; Dong, Y.; Tan, W. Aptasensor with Expanded Nucleotide Using DNA Nanotetrahedra for Electrochemical Detection of Cancerous Exosomes. *ACS Nano* **2017**, *11* (4), 3943−3949.
(116) Zhou, G.; Lin, M.; Song, P.; Chen, X.; Chao, J.; Wang, L.; Huang, Q.; Huang, W.; Fan, C.; Zuo, X. Multivalent Capture and Detection of Cancer Cells with DNA Nanostructured Biosensors and Multibranched Hybridization Chain Reaction Amplification. *Anal. Chem.* **2014**, *86* (15), 7843−7848.
(117) Wang, Z.; Xue, Q.; Tian, W.; Wang, L.; Jiang, W. Quantitative detection of single DNA molecules on DNA tetrahedron decorated substrates. *Chem. Commun.* **2012**, *48* (77), 9661−9663.
(118) Li, W.; Jiang, W.; Ding, Y.; Wang, L. Highly selective and sensitive detection of miRNA based on toehold-mediated strand displacement reaction and DNA tetrahedron substrate. *Biosens. Bioelectron.* **2015**, *71*, 401−406.
(119) Zhang, Y.; Shuai, Z.; Zhou, H.; Luo, Z.; Liu, B.; Zhang, Y.; Zhang, L.; Chen, S.; Chao, J.; Weng, L.; Fan, Q.; Fan, C.; Huang, W.; Wang, L. Single-Molecule Analysis of MicroRNA and Logic Operations Using a Smart Plasmonic Nanobiosensor. *J. Am. Chem. Soc.* **2018**, *140* (11), 3988−3993.
(120) Zeng, D.; Zhang, H.; Zhu, D.; Li, J.; San, L.; Wang, Z.; Wang, C.; Wang, Y.; Wang, L.; Zuo, X.; Mi, X. A novel ultrasensitive electrochemical DNA sensor based on double tetrahedral nanostructures. *Biosens. Bioelectron.* **2015**, *71*, 434−438.
(121) Diao, W.; Tang, M.; Ding, S.; Li, X.; Cheng, W.; Mo, F.; Yan, X.; Ma, H.; Yan, Y. Highly sensitive surface plasmon resonance biosensor for the detection of HIV-related DNA based on dynamic and structural DNA nanodevices. *Biosens. Bioelectron.* **2018**, *100*, 228−234.
(122) Zhang, M.; Jiang, X.-Q.; Le, H.-N.; Wang, P.; Ye, B.-C. Dip-and-read method for label-free renewable sensing enhanced using complex DNA structures. *ACS Appl. Mater. Interfaces* **2013**, *5* (3), 473−478.
(123) Wang, S.; Lu, S.; Zhao, J.; Huang, J.; Yang, X. Real-Time Study of the Interaction between G-Rich DNA Oligonucleotides and Lead Ion on DNA Tetrahedron-Functionalized Sensing Platform by Dual Polarization Interferometry. *ACS Appl. Mater. Interfaces* **2017**, *9* (47), 41568−41576.
(124) Li, Z.; Zhao, B.; Wang, D.; Wen, Y.; Liu, G.; Dong, H.; Song, S.; Fan, C. DNA Nanostructure-Based Universal Microarray Platform for High-Efficiency Multiplex Bioanalysis in Biofluids. *ACS Appl. Mater. Interfaces* **2014**, *6* (20), 17944−17953.
(125) Qu, X.; Zhang, H.; Chen, H.; Aldalbahi, A.; Li, L.; Tian, Y.; Weitz, D. A.; Pei, H. Convection-Driven Pull-Down Assays in Nanoliter Droplets Using Scaffolded Aptamers. *Anal. Chem.* **2017**, *89* (6), 3468−3473.
(126) Qu, X.; Yang, F.; Chen, H.; Li, J.; Zhang, H.; Zhang, G.; Li, L.; Wang, L.; Song, S.; Tian, Y.; Pei, H. Bubble-Mediated Ultrasensitive Multiplex Detection of Metal Ions in Three-Dimensional DNA Nanostructure-Encoded Microchannels. *ACS Appl. Mater. Interfaces* **2017**, *9* (19), 16026−16034.
(127) Schlapak, R.; Danzberger, J.; Armitage, D.; Morgan, D.; Ebner, A.; Hinterdorfer, P.; Pollheimer, P.; Gruber, H. J.; Schäffler, F.; Howorka, S. Nanoscale DNA Tetrahedra Improve Biomolecular Recognition on Patterned Surfaces. *Small* **2012**, *8* (1), 89−97.
(128) Lee, D. S.; Qian, H.; Tay, C. Y.; Leong, D. T. Cellular processing and destinies of artificial DNA nanostructures. *Chem. Soc. Rev.* **2016**, *45* (15), 4199−4225.
(129) Keum, J.-W.; Bermudez, H. Enhanced resistance of DNA nanostructures to enzymatic digestion. *Chem. Commun.* **2009**, *45*, 7036−7038.
(130) Goodman, R. P.; Heilemann, M.; Doose, S.; Erben, C. M.; Kapanidis, A. N.; Turberfield, A. J. Reconfigurable, braced, three-dimensional DNA nanostructures. *Nat. Nanotechnol.* **2008**, *3* (2), 93−96.
(131) Zhou, W.; Li, D.; Xiong, C.; Yuan, R.; Xiang, Y. Multicolor-Encoded Reconfigurable DNA Nanostructures Enable Multiplexed Sensing of Intracellular MicroRNAs in Living Cells. *ACS Appl. Mater. Interfaces* **2016**, *8* (21), 13303−13308.
(132) Li, S.; Xu, L.; Ma, W.; Wu, X.; Sun, M.; Kuang, H.; Wang, L.; Kotov, N. A.; Xu, C. Dual-mode ultrasensitive quantification of microRNA in living cells by chiroplasmonic nanopyramids self-assembled from gold and upconversion nanoparticles. *J. Am. Chem. Soc.* **2016**, *138* (1), 306−312.
(133) Tay, C. Y.; Yuan, L.; Leong, D. T. Nature-inspired DNA nanosensor for real-time in situ detection of mRNA in living cells. *ACS Nano* **2015**, *9* (5), 5609−5617.
(134) He, L.; Lu, D.-Q.; Liang, H.; Xie, S.; Luo, C.; Hu, M.; Xu, L.; Zhang, X.; Tan, W. Fluorescence Resonance Energy Transfer-Based DNA Tetrahedron Nanotweezer for Highly Reliable Detection of Tumor-Related mRNA in Living Cells. *ACS Nano* **2017**, *11* (4), 4060−4066.
(135) He, L.; Lu, D.; Liang, H.; Xie, S.; Zhang, X.; Liu, Q.; Yuan, Q.; Tan, W. mRNA-Initiated, Three-Dimensional DNA Amplifier Able to Function inside Living Cells. *J. Am. Chem. Soc.* **2018**, *140* (1), 258−263.
(136) Xie, N.; Huang, J.; Yang, X.; Yang, Y.; Quan, K.; Wang, H.; Ying, L.; Ou, M.; Wang, K. A DNA tetrahedron-based molecular beacon for tumor-related mRNA detection in living cells. *Chem. Commun.* **2016**, *52* (11), 2346−2349.
(137) Wang, S.; Xia, M.; Liu, J.; Zhang, S.; Zhang, X. Simultaneous Imaging of Three Tumor-Related mRNAs in Living Cells with a DNA Tetrahedron-Based Multicolor Nanoprobe. *ACS Sensors* **2017**, *2* (6), 735−739.
(138) Zhou, W.; Liang, W.; Li, D.; Yuan, R.; Xiang, Y. Dual-color encoded DNAzyme nanostructures for multiplexed detection of

DOI: 10.1021/acssensors.8b00257
ACS Sens. 2018, 3, 903−919

intracellular metal ions in living cells. *Biosens. Bioelectron.* **2016**, *85*, 573−579.
(139) Xie, N.; Huang, J.; Yang, X.; Yang, Y.; Quan, K.; Ou, M.; Fang, H.; Wang, K. Competition-Mediated FRET-Switching DNA Tetrahedron Molecular Beacon for Intracellular Molecular Detection. *ACS Sensors* **2016**, *1* (12), 1445−1452.
(140) Zheng, X.; Peng, R.; Jiang, X.; Wang, Y.; Xu, S.; Ke, G.; Fu, T.; Liu, Q.; Huan, S.; Zhang, X. Fluorescence Resonance Energy Transfer-Based DNA Nanoprism with a Split Aptamer for Adenosine Triphosphate Sensing in Living Cells. *Anal. Chem.* **2017**, *89* (20), 10941−10947.
(141) Feng, Q.-M.; Zhu, M.-J.; Zhang, T.-T.; Xu, J.-J.; Chen, H.-Y. A novel DNA tetrahedron-hairpin probe for in situ ″off-on″ fluorescence imaging of intracellular telomerase activity. *Analyst* **2016**, *141* (8), 2474−2480.
(142) Li, N.; Wang, M.; Gao, X.; Yu, Z.; Pan, W.; Wang, H.; Tang, B. A DNA Tetrahedron Nanoprobe with Controlled Distance of Dyes for Multiple Detection in Living Cells and in Vivo. *Anal. Chem.* **2017**, *89* (12), 6670−6677.
(143) Xie, N.; Huang, J.; Yang, X.; He, X.; Liu, J.; Huang, J.; Fang, H.; Wang, K. Scallop-Inspired DNA Nanomachine: A Ratiometric Nanothermometer for Intracellular Temperature Sensing. *Anal. Chem.* **2017**, *89* (22), 12115−12122.
(144) Yang, F.; Zuo, X.; Fan, C.; Zhang, X.-E. Biomacromolecular nanostructures-based interfacial engineering: from precise assembly to precision biosensing. *Natl. Sci. Rev.* **2018**, DOI: 10.1093/nsr/nwx134.
(145) Li, J.; Fan, C.; Pei, H.; Shi, J.; Huang, Q. Smart Drug Delivery Nanocarriers with Self-Assembled DNA Nanostructures. *Adv. Mater.* **2013**, *25* (32), 4386−4396.
(146) Liang, L.; Li, J.; Li, Q.; Huang, Q.; Shi, J.; Yan, H.; Fan, C. Single-Particle Tracking and Modulation of Cell Entry Pathways of a Tetrahedral DNA Nanostructure in Live Cells. *Angew. Chem., Int. Ed.* **2014**, *53* (30), 7745−7750.
(147) Bellot, G.; McClintock, M. A.; Lin, C.; Shih, W. M. Recovery of intact DNA nanostructures after agarose gel−based separation. *Nat. Methods* **2011**, *8*, 192.
(148) Xing, S.; Jiang, D.; Li, F.; Li, J.; Li, Q.; Huang, Q.; Guo, L.; Xia, J.; Shi, J.; Fan, C.; Zhang, L.; Wang, L. Constructing Higher-Order DNA Nanoarchitectures with Highly Purified DNA Nanocages. *ACS Appl. Mater. Interfaces* **2015**, *7* (24), 13174−13179.
(149) Lin, C.; Perrault, S. D.; Kwak, M.; Graf, F.; Shih, W. M. Purification of DNA-origami nanostructures by rate-zonal centrifugation. *Nucleic Acids Res.* **2013**, *41* (2), e40−e40.
(150) Mathur, D.; Medintz, I. L. Analyzing DNA Nanotechnology: A Call to Arms For The Analytical Chemistry Community. *Anal. Chem.* **2017**, *89* (5), 2646−2663.
(151) Pinheiro, A. V.; Han, D.; Shih, W. M.; Yan, H. Challenges and opportunities for structural DNA nanotechnology. *Nat. Nanotechnol.* **2011**, *6* (12), 763−772.
(152) Zhang, F.; Nangreave, J.; Liu, Y.; Yan, H. Structural DNA Nanotechnology: State of the Art and Future Perspective. *J. Am. Chem. Soc.* **2014**, *136* (32), 11198−11211.
(153) Wang, S.; Deng, S.; Cai, X.; Hou, S.; Li, J.; Gao, Z.; Li, J.; Wang, L.; Fan, C. Superresolution imaging of telomeres with continuous wave stimulated emission depletion (STED) microscope. *Sci. China: Chem.* **2016**, *59* (11), 1519.
(154) Gao, Z.; Deng, S.; Li, J.; Wang, K.; Li, J.; Wang, L.; Fan, C. Sub-diffraction-limit cell imaging using a super-resolution microscope with simplified pulse synchronization. *Sci. China: Chem.* **2017**, *60* (10), 1305−1309.
(155) Chao, J.; Lin, Y.; Liu, H.; Wang, L.; Fan, C. DNA-based plasmonic nanostructures. *Mater. Today* **2015**, *18* (6), 326−335.
(156) Stein, V.; Alexandrov, K. Synthetic protein switches: design principles and applications. *Trends Biotechnol.* **2015**, *33* (2), 101−110.
(157) Jonkheijm, P.; Weinrich, D.; Schröder, H.; Niemeyer, C. M.; Waldmann, H. Chemical strategies for generating protein biochips. *Angew. Chem., Int. Ed.* **2008**, *47* (50), 9618−9647.
(158) Lu, Y.; Aimetti, A. A.; Langer, R.; Gu, Z. Bioresponsive materials. *Nat. Rev. Mater.* **2016**, *2*, 16075.
(159) Zhu, G.; Zheng, J.; Song, E.; Donovan, M.; Zhang, K.; Liu, C.; Tan, W. Self-assembled, aptamer-tethered DNA nanotrains for targeted transport of molecular drugs in cancer theranostics. *Proc. Natl. Acad. Sci. U. S. A.* **2013**, *110* (20), 7998−8003.
(160) Chen, Y.-J.; Groves, B.; Muscat, R. A.; Seelig, G. DNA nanotechnology from the test tube to the cell. *Nat. Nanotechnol.* **2015**, *10*, 748.
(161) Kelley, S. O.; Mirkin, C. A.; Walt, D. R.; Ismagilov, R. F.; Toner, M.; Sargent, E. H. Advancing the speed, sensitivity and accuracy of biomolecular detection using multi-length-scale engineering. *Nat. Nanotechnol.* **2014**, *9* (12), 969−980.
(162) Ye, L.; Yang, F.; Ding, Y.; Yu, H.; Yuan, L.; Dai, Q.; Sun, Y.; Wu, X.; Xiang, Y.; Zhang, G.-J. Bioinspired Trans-Scale Functional Interface for Enhanced Enzymatic Dynamics and Ultrasensitive Detection of microRNA. *Adv. Funct. Mater.* **2018**, *28* (17), 1706981.
(163) Kopperger, E.; List, J.; Madhira, S.; Rothfischer, F.; Lamb, D. C.; Simmel, F. C. A self-assembled nanoscale robotic arm controlled by electric fields. *Science* **2018**, *359* (6373), 296−301.
(164) Kroener, F.; Heerwig, A.; Kaiser, W.; Mertig, M.; Rant, U. Electrical Actuation of a DNA Origami Nanolever on an Electrode. *J. Am. Chem. Soc.* **2017**, *139* (46), 16510−16513.
(165) Yang, F.; Zuo, X.; Li, Z.; Deng, W.; Shi, J.; Zhang, G.; Huang, Q.; Song, S.; Fan, C. A Bubble-Mediated Intelligent Microscale Electrochemical Device for Single-Step Quantitative Bioassays. *Adv. Mater.* **2014**, *26* (27), 4671−4676.
(166) Chin, C. D.; Laksanasopin, T.; Cheung, Y. K.; Steinmiller, D.; Linder, V.; Parsa, H.; Wang, J.; Moore, H.; Rouse, R.; Umviligihozo, G.; Karita, E.; Mwambarangwe, L.; Braunstein, S. L.; van de Wijgert, J.; Sahabo, R.; Justman, J. E.; El-Sadr, W.; Sia, S. K. Microfluidics-based diagnostics of infectious diseases in the developing world. *Nat. Med.* **2011**, *17*, 1015.
(167) Su, Y.; Peng, T.; Xing, F.; Li, D.; Fan, C. Nanoplasmonic Biological Sensing and Imaging. *Huaxue Xuebao* **2017**, *75* (11), 1036−1046.
(168) Long, Y.; Fan, C. Nanosensors. *Acta Chim. Sinica* **2017**, *75*, 1021−1022.
(169) Pei, H.; Zuo, X.; Zhu, D.; Huang, Q.; Fan, C. Functional DNA nanostructures for theranostic applications. *Acc. Chem. Res.* **2014**, *47* (2), 550−559.
(170) Zhu, B.; Wang, L.; Li, J.; Fan, C. Precisely Tailored DNA Nanostructures and their Theranostic Applications. *Chem. Rec.* **2017**, *17* (12), 1213−1230.
(171) Li, S.; Jiang, Q.; Liu, S.; Zhang, Y.; Tian, Y.; Song, C.; Wang, J.; Zou, Y.; Anderson, G. J.; Han, J.-Y.; Chang, Y.; Liu, Y.; Zhang, C.; Chen, L.; Zhou, G.; Nie, G.; Yan, H.; Ding, B.; Zhao, Y. A DNA nanorobot functions as a cancer therapeutic in response to a molecular trigger in vivo. *Nat. Biotechnol.* **2018**, *36*, 258.

DOI: 10.1021/acssensors.8b00257
ACS Sens. 2018, 3, 903−919